Journal of Advances in Applied & Computational Mathematics, 2025, 166-192

Published by Avanti Publishers

Journal of Advances in Applied & Computational Mathematics

ISSN (online): 2409-5761

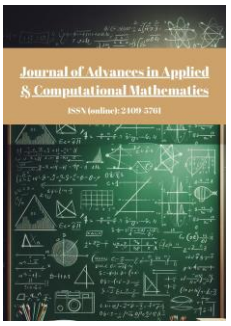

Dynamic Bifurcation Analysis of Incommensurate Fractional-Order Hopfield Neural Networks with Multiple Time Delays

Yiqing Wang[1] and Jun Jiang[2,*]

[1]*College of Science, Wuhan University of Science and Technology, Hubei, China*

[2]*Key Laboratory for Systems Science in Metallurgical Processes, Wuhan University of Science and Technology (WUST), Hubei, China*

ARTICLE INFO

Article Type: Research Article

Academic Editor: Jun Hu

Keywords:
Stability analysis
Nonlinear dynamics
Dynamic bifurcation
Hopfield neural network
Three nonidentical delays
Fractional-order neural networks
Adams-Bashforth-Moulton method

Timeline:
Received: October 22, 2025
Accepted: November 29, 2025
Published: December 28, 2025

Citation: Wang Y, Jiang J. Dynamic bifurcation analysis of incommensurate fractional-order hopfield neural networks with multiple time delays. J Adv Appl Computat Math. 2025; 12: 166-192.

DOI: https://doi.org/10.15377/2409-5761.2025.12.11

ABSTRACT

This study extends a traditional neural network model to an asymmetric Hopfield model incorporating triple time delays through a combined qualitative and quantitative analytical approach. The system is first linearized using Taylor series expansion, followed by the determination of bifurcation points in the resulting system of equations containing quadratic transcendental terms. An improved Adams-Bashforth-Moulton predictor-corrector method is employed for discretization analysis. Theoretical findings are validated through three numerical case studies, with further examination of how time delays influence the system's dynamic behavior.

*Corresponding Author
Email: jiangjun@wust.edu.cn
Tel: +(89) 13147182076

1. Introduction

Fractional calculus generalizes classical integer-order calculus by extending differentiation and integration to arbitrary real orders. Unlike integer-order calculus, which primarily characterizes local properties of functions, fractional calculus incorporates hereditary and memory effects [1]. Consequently, it is widely regarded as an effective tool for describing real-world systems in complex fields such as physics [2], biology [3], and viscoelastic fluids [4]. The distinctive feature of fractional derivatives lies in their nonlocality: the current state of a function depends not only on its instantaneous value but also on its historical states. Although this property poses challenges for computational efficiency, it provides significant advantages in describing natural systems with memory effects. Compared with ordinary differential equation models, fractional differential equation models can more accurately capture the dynamical behavior of complex systems. More importantly, fractional operators can broaden the stability range of systems and delay the occurrence of Hopf bifurcations, making them highly valuable in the study of nonlinear systems and complex networks.

When differential equations involve the historical values of state variables, they give rise to delay differential equations. The fundamental theory and applications of such equations have been systematically studied [5-8]. For example, Matignon [9] investigated the stability of fractional delay differential equations (FDDEs); works [10, 11] analyzed the bounded-input bounded-output stability of linear time-invariant FDDEs. Hwang and Cheng [12] proposed numerical methods for testing FDDE stability, while [13] studied the stability of specific types of FDDEs, and [14] further examined the stability and bifurcation characteristics of generalized FDDEs. In terms of complex dynamical behavior, Bhalekar and Daftardar-Gejji [15] as well as Daftardar-Gejji *et al*. [16] conducted in-depth studies on chaos in FDDEs. Bhalekar [17] revealed chaotic features of different FDDE systems, and in collaboration with others [18, 19], analyzed their applications in nuclear magnetic resonance. These achievements have laid a solid theoretical foundation for the deep integration of fractional-order systems and delays.

In addition to commensurate fractional-order systems, incommensurate fractional differential systems (IFDSs), in which different state variables evolve with distinct fractional orders, have attracted increasing attention. IFDSs can more flexibly describe heterogeneous memory effects and multi-scale dynamics in complex systems, and thus provide a more realistic modeling framework. The well-posedness of general IFDSs was investigated in [20], while [21] studied the existence and uniqueness of mild solutions for incommensurate systems with constant delay. The Ulam–Hyers stability of linear IFDSs was analyzed in [22], and uncertainty analysis of discrete IFDSs in neural networks was examined in [23]. Furthermore, inverse problems and applications of generalized IFDSs were discussed in [24]. These studies collectively highlight the theoretical importance of IFDSs and motivate further investigations into the dynamic behavior of multi-delay incommensurate fractional neural networks.

Early studies on delay-induced dynamics primarily focused on single- and double-delay systems. For instance, Wang [25] developed a stability analysis framework for fractional-order Hopfield neural networks with delays, while Yuan [26] highlighted the significant influence of self-connection delays on bifurcation behaviors. Moreover, references [27-29] investigated the stability regions and Hopf bifurcations of double-delay differential equations. With the advancement of research, multi-delay fractional-order neural networks have attracted increasing attention. In practical systems such as neural networks, communication networks, and distributed control, multi-delay phenomena are widespread, including heterogeneous transmission delays among neural pathways [30], local and long-distance communication delays in networked systems [31], and heterogeneous sensor feedback delays in distributed systems [32]. To address these issues, Li [33] established complete and Mittag-Leffler synchronization criteria for fractional-order neural networks with time-varying delays using Lyapunov methods, Kronecker-product techniques, and adaptive delayed controllers. Ma [34] analyzed Hopf bifurcations in a dual-delay BAM neural network via characteristic equations and root distribution, revealing the effect of fractional order on bifurcation points. Kumar *et al*. [35] and Sivalingam [36] proposed improved L1-based predictor–corrector methods for numerically solving multi-delay fractional-order systems and simulating delay systems with memory effects, providing effective tools for both theoretical analysis and practical applications.

Meanwhile, fractional-order dynamical models, owing to their ability to characterize memory and hereditary properties, have demonstrated substantial advantages in modeling complex real-world systems. Prior work has highlighted the applicability of fractional-order models to disease transmission, biological interactions, and social

behavior dynamics. For instance, the effects of prey refuge and fear factors on the stability and dynamical behavior of a fractional-order predator–prey system were examined in [37]. Fractional differential equations were subsequently employed to investigate the transmission dynamics of lumpy skin disease, along with a systematic evaluation of the effectiveness of quarantine and vaccination strategies [38]. In addition, a Caputo fractional-order model for coffee berry disease was proposed, with analyses of equilibrium stability, existence and uniqueness of solutions, and parameter sensitivity, demonstrating its relevance to plant pathology through numerical simulations [39]. More recently, a social media addiction model incorporating Caputo fractional derivatives and fractal-fractional operators was introduced, establishing existence and uniqueness of solutions as well as Ulam-Hyers stability, and illustrating the potential of fractal-fractional operators in capturing complex social behaviors [40].

Taken together, these studies reveal that fractional-order approaches and multi-delay structures offer significant advantages across ecological systems, epidemiological modeling, and social behavior dynamics. Thus, investigating the multi-delay characteristics of complex systems holds considerable theoretical importance and practical relevance.

It is worth noting that in fractional neural networks, self-connection delay and communication delays are two key types of delays. Self-connection delay refers to the delay caused by the influence of a neuron's own past state on its future evolution. Such delay usually arises from signal processing and transmission times within the neuron, or from computation and feedback mechanisms in artificial neural networks. Existing studies have shown that in second-order recurrent neural networks with delays, suppressing self-connections helps enhance stability and achieve asymptotic convergence [41]. In contrast, communication delay refers to the time required for signal transmission between neurons. This type of delay, particularly pronounced in complex network topologies or long-distance connections, plays a decisive role in synchronization and stability. Wang *et al*. [42], in studying fractional inertial Cohen–Grossberg neural networks, deeply analyzed the impact of time-varying delays on stability and periodic behavior, further highlighting the crucial role of communication delay in neural network dynamics. However, most existing research focuses on single- or double-delay systems. For more realistic systems with three or more delays, theoretical tools and efficient analytical methods remain lacking, due to the presence of multiple transcendental terms in the characteristic equations, the complexity of stability regions, and the difficulty of bifurcation analysis. This issue is especially pronounced when both self-connection and communication delays coexist, since the coupling effects of different types of delays become significant, and traditional dimensionality reduction methods fail to accurately capture the dynamic behavior.

To further explore the dynamic behavior of fractional neural networks with multiple delays, this paper considers a three-delay model consisting of one self-connection delay and two distinct communication delays. For the characteristic equation containing multiple transcendental terms, the classical procedure of multiplying by exponential terms is used to remove delay-related decay factors and facilitate root distribution analysis. The real and imaginary components are then separated to identify the Hopf bifurcation conditions. In this work, Cramer's rule is employed as a convenient algebraic technique to solve the resulting system of equations. Within this established analytical framework, we investigate the stability and bifurcation characteristics of the system and verify the findings through numerical simulations using the predictor–corrector method.

2. Preliminary Knowledge

This section provides a fundamental explanation of the Caputo fractional derivative and its corresponding Laplace transform.

Definition 1 [43] The Caputo fractional order q -th derivative of $f(t)$ is

$$D^q f(t) = \frac{1}{\Gamma(\lceil q \rceil - q)} \int_0^t (t-s)^{\lceil q \rceil - q - 1} f^{(\lceil q \rceil)}(s) ds,$$

where $f \in L^1([0,b])$, $\Gamma(\cdot)$is the Gamma function, q is the fractional orders,$0 < q \leq 1$, $\lceil q \rceil$ is the ceiling of q.

Definition 2 [44] The Laplace transform let $f: [0,\infty) \to R$ be of exponential order, i.e., there exist constants $M > 0$ and $a \in R$ such that

$$|f(t)| \le Me^{at} \quad \forall t \ge 0.$$

Then the integral

$$\mathcal{L}\{f\}(s) := F(s) := \int_0^\infty f(x)e^{-sx}dx$$

converges for all $s > max\{a, 0\}$, and $F(s)$ is called the Laplace transform of f.

Furthermore, let $q > 0$ and set $m := \lceil q \rceil$. If f possesses derivatives up to order $m-1$ on $[0, \infty)$ and $f^{(m-1)}$ is locally absolutely continuous, then for the same range of s satisfies

$$\mathcal{L} \rightleftarrows \{D_0^q f\}(s) = s^q F(s) - \sum_{k=1}^m s^{q-k} f^{(k-1)}(0).$$

In particular, for $y(x) := E_q(-\lambda x^q)$ with $\lambda > 0$, one has

$$L\{y\}(s) = \frac{s^{q-1}}{s^q + \lambda}.$$

Note 1 $\mathcal{L}\{f(t-\sigma)\} = e^{-s\sigma}F(s)$, $\mathcal{L}\{af_1(t) + bf_2(t)\} = aF_1(s) + bF_2(s)$.

Predictor-corrector scheme [45] is a method proposed by Diethelm *et al*. in 2002 for computing fractional order differential equations, also known as the generalized Admas-Bashforth-Moulton method.Its superiority lies in its ability to solve the problem of numerically approximating the solution of general fractional order differential equations.

Consider fractional order time delay differential equation:

$$\begin{cases} D^q x(t) = f_1(t, x(t), x(t-\sigma)), & t \in [0, T], \\ x^{(k)}(t) = g(t), & t \in [-\sigma, 0], \end{cases} \tag{1}$$

where f_1 is a nonlinear function, $q \in (0,1]$, $\sigma > 0$ is the time delay. $h = T/N$,N is sufficiently large, $k = \sigma/h$, k,$N \in Z$, $t_n = nh$, $n = -k, -k+1, \cdots, -1,0,1, \cdots, N$, denote the approximate solution $x_h(t) \approx x(t)$ of equation (1). Then

$$x_h(t_j) = g(t_j), j = -k, -k+1, \cdots, -1,0,$$

the approximate solution of equation (1) containing time delay is

$$x_h(t_j - \sigma) = x_h(jh - kh) = x_h(t_{j-k}), j = 0,1, \cdots, N,$$

substituting the approximate solutionx_h into (1) for integration of order q yields

$$x_h(t_{n+1}) = g(0) + \frac{1}{\Gamma(q)} \int_0^{t_{n+1}} (t_{n+1} - \zeta)^{q-1} f_1(\zeta, x(\zeta), x(\zeta - \sigma)) d\zeta,$$

according to the above equation, from the composite trapezoidal integration formula [46], it can be obtained that

$$\begin{aligned} x_h(t_{n+1}) &= g(0) + \frac{h^q}{\Gamma(q+2)} f_1(t_{n+1}, x_h(t_{n+1}), x_h(t_{n+1} - \sigma)) \\ &\quad + \frac{h^q}{\Gamma(q+2)} \sum_{j=0}^n a_{j,n+1} f_1(t_j, x_h(t_j), x_h(t_j - \sigma)) \\ &= g(0) + \frac{h^q}{\Gamma(q+2)} f_1(t_{n+1}, x_h(t_{n+1}), x_h(t_{n+1-k})) \\ &\quad + \frac{h^q}{\Gamma(q+2)} \sum_{j=0}^n a_{j,n+1} f_1(t_j, x_h(t_j), x_h(t_{j-k})), \end{aligned} \tag{2}$$

of these,

$$a_{j,n+1} = \begin{cases} n^{q+1} - (n-q)(n+1)^q, & j = 0, \\ (n-j+2)^{q+1} + (n-j)^{q+1} - 2(n-j+1)^{q+1}, & 1 \le j \le n, \\ 1, & j = n+1. \end{cases}$$

Since there are $x_h(t_{n+1})$ on both the left and right sides of equation (2) and the function f_1 is nonlinear, it is very difficult to find the solution $x_h(t_{n+1})$ of equation (2). Therefore, the term $x_h(t_{n+1})$ on the right side of equation (2) is replaced by $x_h^P(t_{n+1})$, and $x_h^P(t_{n+1})$ is the prognostic term for the solution $x_h(t_{n+1})$. Applying the composite rectangle rule [47] to the square (1) yields the prediction term

$$\begin{aligned} x_h^P(t_{n+1}) &= g(0) + \frac{1}{\Gamma(q)} \sum_{j=0}^{n} b_{j,n+1} f_1\,(t_j, x_h(t_j), x_h(t_j - \sigma)) \\ &= g(0) + \frac{1}{\Gamma(q)} \sum_{j=0}^{n} b_{j,n+1} f_1\,(t_j, x_h(t_j), x_h(t_{j-k})), \end{aligned}$$

of these,

$$b_{j,n+1} = \frac{h^q}{q}((n+1-j)^q - (n-j)^q).$$

Lemma 1 [21] The m dimensional fractional order linear system without time delay:

$$\begin{cases} D^{\gamma_1} x_1(t) = a_{11}x_1(t) + a_{12}x_2(t) + \cdots + a_{1m}x_m(t), \\ D^{\gamma_2} x_2(t) = a_{21}x_1(t) + a_{22}x_2(t) + \cdots + a_{2m}x_m(t), \\ \vdots \\ D^{\gamma_m} x_m(t) = a_{m1}x_1(t) + a_{m2}x_2(t) + \cdots + a_{mm}x_m(t), \end{cases} \tag{3}$$

$\gamma_i \in (0,1], (i = 1,2,\cdots,m)$, assume that M is the least common multiple of the denominator of $u_1, u_2, \cdots, u_m$, $\gamma_i = \frac{v_i}{u_i}$, $(u_i, v_i) = 1$, $u_i, v_i \in Z^+$, where $i = 1,2,\cdots,m$ and record $r = \frac{1}{M}$. Let $A(\lambda)$ denote the identity matrix of (3)

$$A(\lambda) = \begin{pmatrix} \lambda^{M\gamma_1} - a_{11} & -a_{12} & \cdots & -a_{1m} \\ -a_{21} & \lambda^{M\gamma_2} - a_{22} & \cdots & -a_{2m} \\ \vdots & \vdots & \cdots & \vdots \\ -a_{m1} & a_{m2} & \cdots & \lambda^{M\gamma_m} - a_{mm} \end{pmatrix}$$

then the zero solution of the system (3) is globally asymptotically stable in the Lyapunov sense when all roots λ of the equation $det(A(\lambda)) = 0$ satisfy the condition that all have negative real parts.

The following is an m dimensional linear time delay fractional order system.

Lemma 2 [20] The m dimensional linear time delay fractional order system:

$$\begin{cases} D^{\gamma_1} x_1(t) = a_{11}x_1(t-\sigma_{11}) + \cdots + a_{1m}x_m(t-\sigma_{1m}), \\ D^{\gamma_2} x_2(t) = a_{21}x_1(t-\sigma_{21}) + \cdots + a_{2m}x_m(t-\sigma_{2m}), \\ \vdots \\ D^{\gamma_m} x_m(t) = a_{m1}x_1(t-\sigma_{m1}) + \cdots + a_{mm}x_m(t-\sigma_{mm}), \end{cases} \tag{4}$$

here $\gamma_i \in (0,1]$, $i = 1,2,\cdots,m$, $-max_{ij}\,\sigma_{ij} = -\sigma_{max}$, $\sigma = (\sigma_{ij})_{m\times m} \in (\mathrm{R}^+)^{n\times n}$ denotes the delay matrix, $A = (a_{ij})_{m\times m}$ denotes the coefficient matrix, $x_i(t), x_i(t-\sigma_{ij}) \in \mathrm{R}$ denotes the state variables, $x_i(t) \in C[-\sigma_{max}$,Laplace transforms on each side of the system (4).

$$\begin{cases} \mathcal{L}(D^{\gamma_1} x_1(t)) = \mathcal{L}[a_{11}x_1(t-\sigma_{11}) + \cdots + a_{1m}x_m(t-\sigma_{1m})], \\ \mathcal{L}(D^{\gamma_2} x_2(t)) = \mathcal{L}[a_{21}x_1(t-\sigma_{21}) + \cdots + a_{2m}x_m(t-\sigma_{2m})], \\ \vdots \\ \mathcal{L}(D^{\gamma_m} x_m(t)) = \mathcal{L}[a_{m1}x_1(t-\sigma_{m1}) + \cdots + a_{mm}x_m(t-\sigma_{mm})], \end{cases}$$

From the definition and properties of the Laplace transform, it follows that

$$\begin{cases} s^{\gamma_1}X_1(s) = a_{11}e^{-s\sigma_{11}}X_1(s) + \cdots + a_{1m}e^{-s\sigma_{1m}}X_m(s), \\ s^{\gamma_2}X_2(s) = a_{21}e^{-s\sigma_{21}}X_1(s) + \cdots + a_{2m}e^{-s\sigma_{2m}}X_m(s), \\ \vdots \\ s^{\gamma_m}X_m(s) = a_{m1}e^{-s\sigma_{m1}}X_1(s) + \cdots + a_{mm}e^{-s\sigma_{mm}}X_m(s), \end{cases}$$

Consequently,

$$\begin{pmatrix} s^{\gamma_1} - a_{11}e^{-s\sigma_{11}} & \cdots & -a_{1m}e^{-s\sigma_{1m}} \\ -a_{21}e^{-s\sigma_{21}} & \cdots & -a_{2m}e^{-s\sigma_{2m}} \\ \vdots & \vdots & \vdots \\ -a_{m1}e^{-s\sigma_{m1}} & \cdots & s^{\gamma_m} - a_{mm}e^{-s\sigma_{mm}} \end{pmatrix} \begin{pmatrix} X_1(s) \\ X_2(s) \\ \vdots \\ X_m(s) \end{pmatrix} = 0.$$

The identity matrix of system (4) is defined as S:

$$S = \begin{pmatrix} s^{\gamma_1} - a_{11}e^{-s\sigma_{11}} & \cdots & -a_{1m}e^{-s\sigma_{1n}} \\ -a_{21}e^{-s\sigma_{21}} & \cdots & -a_{2m}e^{-s\sigma_{2m}} \\ \vdots & \vdots & \vdots \\ -a_{m1}e^{-s\sigma_{m1}} & \cdots & s^{\gamma_m} - a_{mm}e^{-s\sigma_{mm}} \end{pmatrix}.$$

If all roots s of the characteristic equation $det(S) = 0$ have negative real parts, then the zero solution of the system (4) is Lyapunov globally asymptotically stable.

3. Model Descriptions

This section describes a three-neuron, three-delay fully connected neural network sustem (5). The system takes into account both instantaneous and delayed interactions between neurons, effectively simulating complex systems with memory and long-term dependencies.

$$\begin{cases} D^{\gamma_1}y_1(t) &= -p_1y_1(t) + \iota_1M_1(y_1(t-\sigma_1)) + \rho_1N_1(y_2(t-\sigma_2)) \\ &\quad +\kappa_1T_1(y_3(t-\sigma_3)), \\ D^{\gamma_2}y_2(t) &= -p_2y_2(t) + \iota_2M_2(y_2(t-\sigma_1)) + \rho_2N_2(y_3(t-\sigma_2)) \\ &\quad +\kappa_2T_2(y_1(t-\sigma_3)), \\ D^{\gamma_3}y_3(t) &= -p_3y_3(t) + \iota_3M_3(y_3(t-\sigma_1)) + \rho_3N_3(y_1(t-\sigma_2)) \\ &\quad +\kappa_3T_3(y_2(t-\sigma_3)), \end{cases} \tag{5}$$

$\gamma_i \in (0,1], (i = 1,2,3)$ denotes the fractional order order, $y_i(t)$ indicates the neuron node, $p_i > 0$ is called the neuron autotuning parameter, ι_i, ρ_i and $\kappa_i \in R$ are the connection weight, $M_i(\cdot), N_i(\cdot), T_i(\cdot)$denotes the activation function, $\sigma_1 \geq 0$ denotes the self-connection time delay, $\sigma_2 \geq 0$ and $\sigma_3 \geq 0$ are different communication delays in the system.

The structure of system (5) is shown in Fig. (**1**).

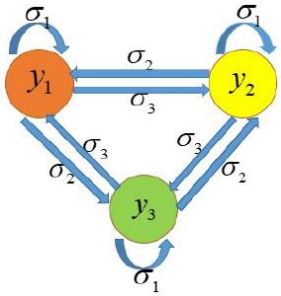

Figure 1: Topological structure of fractional order neural network system.

The main objective of this paper is to establish Hopf bifurcation of fractional order neural network system with three-time delays to investigate the influence mechanism of time delay combination on the bifurcation point of the network and to consider the influence of time delay and order on the stability of the system so that the precise stability intervals and bifurcation conditions are obtained.

Usually, in order to reduce the difficulty of numerical analysis and numerical simulation, we need to make some assumptions about some state variables.

Hypothesis 1 $M_i(\cdot), N_i(\cdot), T_i(\cdot) \in C^1(\mathrm{R}, \mathrm{R})$,$M_i(0) = N_i(0) = T_i(0) = 0$.

The activation functions $M_i(\cdot), N_i(\cdot), T_i(\cdot)$are assumed to be bounded, continuously differentiable, monotone increasing sigmoid-type functions, and satisfy the Lipschitz condition.

In the numerical simulation part, we choose $tanh(\cdot)$ as the specific activation function. Since $tanh(\cdot)$ is bounded, smooth, monotone, and Lipschitz continuous, it fully satisfies the above assumptions, thereby ensuring consistency between the theoretical analysis and the simulation results.

Under the given conditions, system (5) has a zero equilibrium point. This assumption is commonly used in neural network analysis for convenience. For neural networks with a non-zero equilibrium point, a coordinate shift can be applied to transform it into a zero equilibrium point, facilitating further analysis.

For any activation function $M_i(\cdot)$, its Taylor expansion around the equilibrium point 0 (retaining the first-order term) can be written as

$$M_i(y_j(t-\sigma_j)) = M_i(0) + M_{i'}(0)y_j(t-\sigma_j) + o\big(y_j(t-\sigma_j)\big).$$

If the equilibrium is at the origin and we assume $M_i(0) = 0$ (which holds for odd-symmetric sigmoids such as $tanh$), then the constant term vanishes and the linearized approximation becomes

$$M_i(y_j(t-\sigma_j)) \approx \ell_i y_j(t-\sigma_j).$$

Simarily

$$\begin{aligned} M_i(y_j(t-\sigma_j)) &\approx \wp_i y_j(t-\sigma_j), \\ M_i(y_j(t-\sigma_j)) &\approx x_i y_j(t-\sigma_j). \end{aligned}$$

hereby, $\ell_i = \iota_i M_i{}'(0)$. $\wp_i = \rho_i N_i{}'(0)$, $x_i = \kappa_i T_i{}'(0) (i = 1,2,3)$.

Linearising at the origin of system (5) and using the Taylor expansion yields

$$\begin{cases} D^{\gamma_1} y_1(t) &= -p_1 y_1(t) + \ell_1 y_1(t-\sigma_1) + \wp_1 y_2(t-\sigma_2) \\ &\quad + x_1 y_3(t-\sigma_3), \\ D^{\gamma_2} y_2(t) &= -p_2 y_2(t) + \ell_2 y_2(t-\sigma_1) + \wp_2 y_3(t-\sigma_2) \\ &\quad + x_2 y_1(t-\sigma_3), \\ D^{\gamma_3} y_3(t) &= -p_3 y_3(t) + \ell_3 y_3(t-\sigma_1) + \wp_3 y_1(t-\sigma_2) \\ &\quad + x_3 y_2(t-\sigma_3), \end{cases} \tag{6}$$

Good results have been achieved after linearisation with this method in many articles, such as solving fractional-order binary delay Cohen-Grossberg neural networks [48], fractional order dynamic model of genetic regulatory networks with delays [49], etc.

4. Main Results

In order to study the local stability of fractional order neural network system (5) and to obtain the bifurcation conditions, this section will be divided into the following seven cases according to a linear system (6).

Situation 1$\sigma_1 = \sigma_2 = \sigma_3 = 0$

For $\sigma_1 = \sigma_2 = \sigma_3 = 0$, the linear system (6) reduces to system (7) without a time delay, as shown below.

$$\begin{cases} D^{\gamma_1} y_1(t) = -p_1 y_1(t) + \ell_1 y_1(t) + \wp_1 y_2(t) + x_1 y_3(t), \\ D^{\gamma_2} y_2(t) = -p_2 y_2(t) + \ell_2 y_2(t) + \wp_2 y_3(t) + x_2 y_1(t), \\ D^{\gamma_3} y_3(t) = -p_3 y_3(t) + \ell_3 y_3(t) + \wp_3 y_1(t) + x_3 y_2(t). \end{cases} \tag{7}$$

The identity matrix of (7) is:

$$\begin{pmatrix} s^{\gamma_1} + p_1 - \ell_1 & -\wp_1 & -x_1 \\ -x_2 & s^{\gamma_2} + p_2 - \ell_2 & -\wp_2 \\ -\wp_3 & -x_3 & s^{\gamma_3} + p_3 - \ell_2 \end{pmatrix},$$

under the condition that $\sigma_1 = \sigma_2 = \sigma_3 = 0$, system (6) is asymptotically stable if all the roots of $det(S) = 0$ satisfy the conditions of Lemma 1.

Situation 2$\sigma_1 > 0, \sigma_2 = \sigma_3 = 0$

If $\sigma_1 > 0, \sigma_2 = \sigma_3 = 0$, then (6) becomes a single time delay system (8) as follows

$$\begin{cases} D^{\gamma_1} y_1(t) = -p_1 y_1(t) + \ell_1 y_1(t - \sigma_1) + \wp_1 y_2(t) + x_1 y_3(t), \\ D^{\gamma_2} y_2(t) = -p_2 y_2(t) + \ell_2 y_2(t - \sigma_1) + \wp_2 y_3(t) + x_2 y_1(t), \\ D^{\gamma_3} y_3(t) = -p_3 y_3(t) + \ell_3 y_3(t - \sigma_1) + \wp_3 y_1(t) + x_3 y_2(t), \end{cases} \tag{8}$$

The identity matrix of single time delay system (8) is

$$\begin{pmatrix} s^{\gamma_1} + p_1 - \ell_1 e^{-s\sigma_1} & -\wp_1 & -x_1 \\ -x_2 & s^{\gamma_2} + p_2 - \ell_2 e^{-s\sigma_1} & -\wp_2 \\ -\wp_3 & -x_3 & s^{\gamma_3} + p_3 - \ell_3 e^{-s\sigma_1} \end{pmatrix}.$$

The characteristic equation of system (8) is

$$\mathrm{A}_0(s) + \mathrm{A}_1(s) e^{-s\sigma_1} + \mathrm{A}_2(s) e^{-2s\sigma_1} + \mathrm{A}_3(s) e^{-3s\sigma_1} = 0, \tag{9}$$

Of these,

$$\begin{aligned} \mathrm{A}_0(s) = \; & s^{\gamma_1+\gamma_2+\gamma_3} + p_3 s^{\gamma_1+\gamma_2} + p_2 s^{\gamma_1+\gamma_3} + p_1 s^{\gamma_2+\gamma_3} \\ & + p_2 p_3 s^{\gamma_1} + p_1 p_3 s^{\gamma_2} + p_1 p_2 s^{\gamma_3} + p_1 p_2 p_3 \\ & - \wp_1 \wp_2 \wp_3 - x_1 x_2 x_3 \\ & - \wp_3 x_1 s^{\gamma_2} - \wp_3 p_2 x_1 - \wp_1 x_2 s^{\gamma_3} \\ & - \wp_1 p_3 x_2 - \wp_2 x_3 s^{\gamma_1} - \wp_2 p_1 x_3 \end{aligned}$$

$$\begin{aligned} \mathrm{A}_1(s) = \; & -\ell_3 s^{\gamma_1+\gamma_2} - \ell_2 s^{\gamma_1+\gamma_3} - \ell_1 s^{\gamma_2+\gamma_3} \\ & - (p_2 \ell_1 + p_3 \ell_2) s^{\gamma_1} - (p_1 \ell_3 + p_3 \ell_1) s^{\gamma_2} \\ & - (p_1 \ell_2 + p_2 \ell_1) s^{\gamma_3} \\ & - p_1 p_2 \ell_3 + p_1 p_3 \ell_2 + p_2 p_3 \ell_1 \\ & - \wp_3 \ell_2 x_1 - \wp_1 \ell_3 x_2 - \wp_1 p_2 \ell_3 - \wp_2 \ell_1 x_3 \end{aligned}$$

$$\begin{aligned} \mathrm{A}_2(s) = \; & \ell_2 \ell_3 s^{\gamma_1} + \ell_1 \ell_3 s^{\gamma_2} + \ell_1 \ell_2 s^{\gamma_3} \\ & + p_3 \ell_1 \ell_2 + p_2 \ell_1 \ell_3 + p_1 \ell_2 \ell_3 \end{aligned}$$

$$\mathrm{A}_3(s) = -\ell_1 \ell_2 \ell_3.$$

Wang [50] formulate an expression for the bifurcation point of a characteristic equation containing any order transcendental function utilizing the eigenvalue distribution method.

Multiply both sides of the equation (9) by $e^{s\sigma_1}$ and $e^{2s\sigma_1}$

$$\begin{cases} \mathrm{A}_0(s)e^{s\sigma_1} + \mathrm{A}_1(s) + \mathrm{A}_2(s)e^{-s\sigma_1} + \mathrm{A}_3(s)e^{-2s\sigma_1} = 0, \\ \mathrm{A}_0(s)e^{2s\sigma_1} + \mathrm{A}_1(s)e^{s\sigma_1} + \mathrm{A}_2(s) + \mathrm{A}_3(s)e^{-s\sigma_1} = 0. \end{cases} \tag{10}$$

According to the condition for a Hopf bifurcation in the system from reference [51], we set $s = \overline{\omega}\left(cos\frac{\pi}{2} + i\,sin\frac{\pi}{2}\right)$, $(\overline{\omega} > 0)$, and insert s into (10). By Euler's formula, we have

$$s^q = (\overline{\omega}i)^q = \overline{\omega}^q e^{iq\pi/2} = \overline{\omega}^q\,[\,cos\left(\frac{q\pi}{2}\right) + i\,sin\left(\frac{q\pi}{2}\right)].$$

here, $\omega, q \in R$. Therefore, the real and imaginary parts of s^q are given respectively by

$$\overline{\omega}^q\,cos\left(\frac{q\pi}{2}\right) \quad \text{and} \quad \overline{\omega}^q\,sin\left(\frac{q\pi}{2}\right).$$

For brevity, we let A_i^R, A_i^I denote the real and imaginary parts of $A_i(s)$, $(i = 0,1,2,3)$, respectively, which can then be obtained.

$$\begin{cases} \mathfrak{C}_{11}\,cos\,\overline{\omega}\,\sigma_1 + \mathfrak{C}_{12}\,sin\,\overline{\omega}\,\sigma_1 + \mathfrak{C}_{13}\,cos\,2\,\overline{\omega}\sigma_1 + \mathfrak{C}_{14}\,sin\,2\,\overline{\omega}\sigma_1 = -\mathrm{A}_1{}^R, \\ \mathfrak{C}_{21}\,cos\,\overline{\omega}\,\sigma_1 + \mathfrak{C}_{22}\,sin\,\overline{\omega}\,\sigma_1 + \mathfrak{C}_{23}\,cos\,2\,\overline{\omega}\sigma_1 + \mathfrak{C}_{24}\,sin\,2\,\overline{\omega}\sigma_1 = -\mathrm{A}_1{}^I, \\ \mathfrak{C}_{31}\,cos\,\overline{\omega}\,\sigma_1 + \mathfrak{C}_{32}\,sin\,\overline{\omega}\,\sigma_1 + \mathfrak{C}_{33}\,cos\,2\,\overline{\omega}\sigma_1 + \mathfrak{C}_{34}\,sin\,2\,\overline{\omega}\sigma_1 = -\mathrm{A}_2{}^R, \\ \mathfrak{C}_{41}\,cos\,\overline{\omega}\,\sigma_1 + \mathfrak{C}_{42}\,sin\,\overline{\omega}\,\sigma_1 + \mathfrak{C}_{43}\,cos\,2\,\overline{\omega}\sigma_1 + \mathfrak{C}_{44}\,sin\,2\,\overline{\omega}\sigma_1 = -\mathrm{A}_2{}^I, \end{cases} \tag{11}$$

here

$$\begin{cases} \mathfrak{C}_{11} = \mathrm{A}_0{}^R + \mathrm{A}_2{}^R, \quad \mathfrak{C}_{12} = \mathrm{A}_2{}^I - \mathrm{A}_0{}^I, \quad \mathfrak{C}_{13} = \mathrm{A}_3{}^R, \quad \mathfrak{C}_{14} = \mathrm{A}_3{}^I, \\ \mathfrak{C}_{21} = \mathrm{A}_0{}^I + \mathrm{A}_2{}^I, \quad \mathfrak{C}_{22} = \mathrm{A}_0{}^R - \mathrm{A}_2{}^R, \quad \mathfrak{C}_{23} = \mathrm{A}_3{}^I, \quad \mathfrak{C}_{24} = -\mathrm{A}_3{}^R, \\ \mathfrak{C}_{31} = \mathrm{A}_1{}^R + \mathrm{A}_3{}^R, \quad \mathfrak{C}_{32} = \mathrm{A}_3{}^I - \mathrm{A}_1{}^I, \quad \mathfrak{C}_{33} = \mathrm{A}_0{}^R, \quad \mathfrak{C}_{34} = -\mathrm{A}_0{}^I, \\ \mathfrak{C}_{41} = \mathrm{A}_1{}^I + \mathrm{A}_3{}^I, \quad \mathfrak{C}_{42} = \mathrm{A}_1{}^R - \mathrm{A}_3{}^R, \quad \mathfrak{C}_{43} = \mathrm{A}_0{}^I, \quad \mathfrak{C}_{44} = \mathrm{A}_0{}^R. \end{cases}$$

The determinant of coefficient of equations (11) can be expressed as follows:

$$\mathrm{C} = \begin{vmatrix} \mathfrak{C}_{11} & \mathfrak{C}_{12} & \mathfrak{C}_{13} & \mathfrak{C}_{14} \\ \mathfrak{C}_{21} & \mathfrak{C}_{22} & \mathfrak{C}_{23} & \mathfrak{C}_{24} \\ \mathfrak{C}_{31} & \mathfrak{C}_{32} & \mathfrak{C}_{33} & \mathfrak{C}_{34} \\ \mathfrak{C}_{41} & \mathfrak{C}_{42} & \mathfrak{C}_{43} & \mathfrak{C}_{44} \end{vmatrix}.$$

To ensure the existence and uniqueness of solutions to system (8), the coefficient matrix in equation (11) should be non-singular.

To further establish the bifurcation point with respect to σ_1, the expressions for $cos\,\omega\,\sigma_1$ and $sin\,\omega\,\sigma_1$ can be computed using Cramer's law

$$\begin{cases} cos(\,\overline{\omega}\sigma_1) = \frac{\mathfrak{C}_1}{\mathfrak{C}} = \overline{\Psi_1}(\overline{\omega}), \\ sin(\,\overline{\omega}\sigma_1) = \frac{\mathfrak{C}_2}{\mathfrak{C}} = \overline{\Psi_2}(\overline{\omega}) \end{cases} \tag{12}$$

in

$$\mathfrak{C}_1 = \begin{vmatrix} -\mathrm{A}_1{}^R & \mathfrak{C}_{12} & \mathfrak{C}_{13} & \mathfrak{C}_{14} \\ -\mathrm{A}_1{}^I & \mathfrak{C}_{22} & \mathfrak{C}_{23} & \mathfrak{C}_{24} \\ -\mathrm{A}_2{}^R & \mathfrak{C}_{32} & \mathfrak{C}_{33} & \mathfrak{C}_{34} \\ -\mathrm{A}_2{}^I & \mathfrak{C}_{42} & \mathfrak{C}_{43} & \mathfrak{C}_{44} \end{vmatrix}, \mathfrak{C}_2 = \begin{vmatrix} \mathfrak{C}_{11} & -\mathrm{A}_1{}^R & \mathfrak{C}_{13} & \mathfrak{C}_{14} \\ \mathfrak{C}_{21} & -\mathrm{A}_1{}^I & \mathfrak{C}_{23} & \mathfrak{C}_{24} \\ \mathfrak{C}_{31} & -\mathrm{A}_2{}^R & \mathfrak{C}_{33} & \mathfrak{C}_{34} \\ \mathfrak{C}_{41} & -\mathrm{A}_2{}^I & \mathfrak{C}_{43} & \mathfrak{C}_{44} \end{vmatrix},$$

From equation (12) it is clear that

$$\overline{\Psi_1}^2(\overline{\omega}) + \overline{\Psi_2}^2(\overline{\omega}) = 1 \tag{13}$$

Hypothesis 2 There are positive real roots in equation (13).

From the first equation in the system of equations (12), we can see that

$$\overline{\sigma_{1k}} = \frac{1}{\overline{\omega}}[arccos(\overline{\Psi_1}(\overline{\omega})) + 2k\pi], \quad k = 0,1,2,\cdots \tag{14}$$

Define the first bifurcation point of system (8) as

$$\overline{\sigma_{10}} = min\{\overline{\sigma_{10}}, \overline{\sigma_{11}}, \dots, \overline{\sigma_{1k}}, \dots\} = \frac{1}{\overline{\omega}} arccos(\overline{\Psi_1}(\overline{\omega}))$$

Hypothesis 3 $\frac{-H_{\sigma_1}{}^R H_s{}^R - H_{\sigma_1}{}^I H_s{}^I}{(H_s{}^R)^2 + (H_s{}^I)^2} \neq 0$, where $H_{\sigma_1}{}^R, H_{\sigma_1}{}^I$,

$H_s{}^R, H_s{}^I$ are the real and imaginary parts of H_{σ_1} and H_s respectively, with H_{σ_1} and H_s described in the following equation (10).

Lemma 3 $s(\sigma_1) = \mu(\sigma_1) + i\overline{\omega}(\sigma_1)$ be a solution of equation(9) satisfying $\mu(\overline{\sigma_{10}}) = 0$, $\overline{\omega}(\overline{\sigma_{10}}) = \overline{\omega_0}$ near $\sigma_1 = \overline{\sigma_{10}}$. Then the following transversality condition holds

$$Re\left[\frac{ds}{d\sigma_1}\right]\Big|_{(\bar{\omega}=\overline{\omega_0}, \sigma_1=\overline{\sigma_{10}})} \neq 0$$

Proof

Let $H(s, \sigma_1) = \mathrm{A}_0(s) + \mathrm{A}_1(s)e^{-s\sigma_1} + \mathrm{A}_2(s)e^{-2s\sigma_1} + \mathrm{A}_3(s)e^{-3s\sigma_1}$. By the implicit function theorem, the equation is differentiable with respect to σ_1:

$$\frac{ds}{d\sigma_1} = -\frac{H_{\sigma_1}}{H_s}, \tag{15}$$

$$\begin{aligned} H_{\sigma_1} &= -s[\mathrm{A}_1(s)e^{-s\sigma_1} + 2\mathrm{A}_2(s)e^{-2s\sigma_1} + 3\mathrm{A}_3(s)e^{-3s\sigma_1}], \\ H_s &= \mathrm{A}_0{}'(s) + [\mathrm{A}_1{}'(s) - \sigma_1\mathrm{A}_1(s)]e^{-s\sigma_1} \\ &\quad + [\mathrm{A}_2{}'(s) - 2\sigma_1\mathrm{A}_2(s)]e^{-2s\sigma_1} \\ &\quad + [\mathrm{A}_3{}'(s) - 3\sigma_1\mathrm{A}_3(s)]e^{-3s\sigma_1}. \end{aligned}$$

Based on equation (15), we can deduce

$$\begin{aligned} \frac{ds}{d\sigma_1} &= -\frac{H_{\sigma_1}}{H_s} \\ &= -\frac{H_{\sigma_1}{}^R + iH_{\sigma_1}{}^I}{H_s{}^R + iH_s{}^I} \\ &= \frac{(-H_{\sigma_1}{}^R - iH_{\sigma_1}{}^I)(H_s{}^R - iH_s{}^I)}{(H_s{}^R)^2 + (H_s{}^I)^2} \\ &= \frac{-H_{\sigma_1}{}^R H_s{}^R - H_{\sigma_1}{}^I H_s{}^I}{(H_s{}^R)^2 + (H_s{}^I)^2} + i\frac{H_{\sigma_1}{}^R H_s{}^I - H_{\sigma_1}{}^I H_s{}^R}{(H_s{}^R)^2 + (H_s{}^I)^2}, \end{aligned}$$

therefore,

$$Re\left[\frac{ds}{d\sigma_1}\right]\Big|_{(\bar{\omega}=\overline{\omega_0}, \sigma_1=\overline{\sigma_{10}})} = \frac{-H_{\sigma_1}{}^R H_s{}^R - H_{\sigma_1}{}^I H_s{}^I}{(H_s{}^R)^2 + (H_s{}^I)^2}.$$

Let $A_i{}'^R$ and $A_i{}'^I$ be the real and imaginary parts of $A_i{}'$, and $A_i{}^R$ and $A_i{}^I$ be the real and imaginary parts of A_i,

respectively.

$$\begin{aligned}
H^R_{\sigma_1} &= -\overline{\omega_0}[\mathrm{A}^R_1 sin(\overline{\omega_0\sigma_{10}}) - \mathrm{A}^I_1 cos(\overline{\omega_0\sigma_{10}}) \\
&\quad +2\mathrm{A}^R_2 sin(2\overline{\omega_0\sigma_{10}}) - 2\mathrm{A}^I_2 cos(2\overline{\omega_0\sigma_{10}}) \\
&\quad +3\mathrm{A}^R_3 sin(3\overline{\omega_0\sigma_{10}}) - 3\mathrm{A}^I_3 cos(3\overline{\omega_0\sigma_{10}})] \\
H^I_{\sigma_1} &= -\overline{\omega_0}[\mathrm{A}^R_1 cos(\overline{\omega_0\sigma_{10}}) + \mathrm{A}^I_1 sin(\overline{\omega_0\sigma_{10}}) \\
&\quad +2\mathrm{A}^R_2 cos(2\overline{\omega_0\sigma_{10}}) + 2\mathrm{A}^I_2 sin(2\overline{\omega_0\sigma_{10}}) \\
&\quad +3\mathrm{A}^R_3 cos(3\overline{\omega_0\sigma_{10}}) + 3\mathrm{A}^I_3 sin(3\overline{\omega_0\sigma_{10}})] \\
H^R_s &= \mathrm{A}'^R_0 + (\mathrm{A}'^R_1 - \overline{\sigma_{10}}\mathrm{A}^R_1) cos(\overline{\omega_0\sigma_{10}}) \\
&\quad +(\mathrm{A}'^I_1 - \overline{\sigma_{10}}\mathrm{A}^I_1) sin(\overline{\omega_0\sigma_{10}}) \\
&\quad +(\mathrm{A}'^R_2 - 2\overline{\sigma_{10}}\mathrm{A}^R_2) cos(2\overline{\omega_0\sigma_{10}}) \\
&\quad +(\mathrm{A}'^I_2 - 2\overline{\sigma_{10}}\mathrm{A}^I_2) sin(2\overline{\omega_0\sigma_{10}}) \\
&\quad +(\mathrm{A}'^R_3 - 3\overline{\sigma_{10}}\mathrm{A}^R_3) cos(3\overline{\omega_0\sigma_{10}}) \\
&\quad +(\mathrm{A}'^I_3 - 3\overline{\sigma_{10}}\mathrm{A}^I_3) sin(3\overline{\omega_0\sigma_{10}}) \\
H^I_s &= \mathrm{A}'^I_0 + (\mathrm{A}'^I_1 - \overline{\sigma_{10}}\mathrm{A}^I_1) cos(\overline{\omega_0\sigma_{10}}) \\
&\quad +(\overline{\sigma_{10}}\mathrm{A}^R_1 - \mathrm{A}'^R_1) sin(\overline{\omega_0\sigma_{10}}) \\
&\quad +(\mathrm{A}'^I_2 - 2\overline{\sigma_{10}}\mathrm{A}^I_2) cos(2\overline{\omega_0\sigma_{10}}) \\
&\quad +(2\overline{\sigma_{10}}\mathrm{A}^R_2 - \mathrm{A}'^R_2) sin(2\overline{\omega_0\sigma_{10}}) \\
&\quad +(\mathrm{A}'^I_3 - 3\overline{\sigma_{10}}\mathrm{A}^I_3) cos(3\overline{\omega_0\sigma_{10}}) \\
&\quad +(3\overline{\sigma_{10}}\mathrm{A}^R_3 - \mathrm{A}'^R_3) sin(3\overline{\omega_0\sigma_{10}})
\end{aligned}$$

Given Hypothesis 3 and the applicability of Lemma 2, it follows that a Hopf bifurcation occurs at $\sigma_1 = \overline{\sigma_{10}}$, where the stability range is $[0, \overline{\sigma_{10}})$.

Situation 3 $\sigma_2 > 0, \sigma_1 = \sigma_3 = 0$

If $\sigma_2 > 0, \sigma_1 = \sigma_3 = 0$, system (6) is transformed into a single time delay system (16) as follows

$$\begin{cases} D^{\gamma_1}y_1(t) = -p_1y_1(t) + \ell_1y_1(t) + \mathrm{p}_1y_2(t-\sigma_2) + x_1y_3(t), \\ D^{\gamma_2}y_2(t) = -p_2y_2(t) + \ell_2y_2(t) + \mathrm{p}_2y_3(t-\sigma_2) + x_2y_1(t), \\ D^{\gamma_3}y_3(t) = -p_3y_3(t) + \ell_3y_3(t) + \mathrm{p}_3y_1(t-\sigma_2) + x_3y_2(t), \end{cases} \tag{16}$$

the identity matrix of single time delay system (16) is:

$$\begin{pmatrix} s^{\gamma_1} + p_1 - \ell_1 & -\wp_1 e^{-s\sigma_2} & -x_1 \\ -x_2 & s^{\gamma_2} + p_2 - \ell_2 & -\wp_2 e^{-s\sigma_2} \\ -\wp_3 e^{-s\sigma_2} & -x_3 & s^{\gamma_3} + p_3 - \ell_3 \end{pmatrix}.$$

The characteristic equation of system (16) is as follows

$$\mathrm{B}_0(s) + \mathrm{B}_1(s)e^{-s\sigma_2} + \mathrm{B}_2(s)e^{-2s\sigma_2} + \mathrm{B}_3(s)e^{-3s\sigma_2} = 0, \tag{17}$$

Where

$$\begin{aligned}
\mathrm{B}_0(s) = \; & s^{\gamma_1+\gamma_2+\gamma_3} + (p_3 - \ell_3)s^{\gamma_1+\gamma_2} + (p_2 - \ell_2)s^{\gamma_1+\gamma_3} + (p_1 - \ell_1)s^{\gamma_2+\gamma_3} \\
& +(p_2p_3 - p_2\ell_3 - p_3\ell_2 + \ell_2\ell_3)s^{\gamma_1} \\
& +(p_1p_3 - p_1\ell_3 - p_3\ell_1 + \ell_1\ell_3)s^{\gamma_2} \\
& +(p_1p_2 - p_1\ell_2 - p_2\ell_1 + \ell_1\ell_2)s^{\gamma_3} \\
& +p_1p_2p_3 - p_1p_2\ell_3 - p_1p_3\ell_2 + p_1\ell_2\ell_3 \\
& -p_2p_3\ell_1 + p_2\ell_1\ell_3 + p_3\ell_1\ell_2 - \ell_1\ell_2\ell_3 - x_1x_2x_3 \\
\mathrm{B}_1(s) = \; & -\wp_3x_1(s^{\gamma_2} + p_2 - \wp_2) - \wp_1x_2(s^{\gamma_3} + p_3 - \ell_3) \\
& -\wp_2x_3(s^{\gamma_1} + p_1 - \ell_1)
\end{aligned}$$

$$\mathrm{B}_2(s) = 0, \quad \mathrm{B}_3(s) = -\wp_1\wp_2\wp_3.$$

Equation (17) is multiplied by $e^{s\sigma_2}$, $e^{2s\sigma_2}$ on both sides

$$\begin{cases} \mathrm{B}_0(s)e^{s\sigma_2} + \mathrm{B}_1(s) + \mathrm{B}_2(s)e^{-s\sigma_2} + \mathrm{B}_3(s)e^{-2s\sigma_2} = 0, \\ \mathrm{B}_0(s)e^{2s\sigma_2} + \mathrm{B}_1(s)e^{s\sigma_2} + \mathrm{B}_2(s) + \mathrm{B}_3(s)e^{-s\sigma_2} = 0. \end{cases} \tag{18}$$

Let $s = \hat{\omega}\left(cos\frac{\pi}{2} + i\,sin\frac{\pi}{2}\right), \quad (\hat{\omega} > 0)$ be the positive imaginary root of the system of equations (18).

For simplicity, the real and imaginary parts of $B_i(s)$ $(i = 0,1,2,3)$ are denoted by

$$\mathrm{B}_i^R \quad \text{and} \quad \mathrm{B}_i^I,$$

respectively. It can then be obtained that …

$$\begin{cases} \Xi_{11}\,cos\,\hat{\omega}\,\sigma_2 + \Xi_{12}\,sin\,\hat{\omega}\,\sigma_2 + \Xi_{13}\,cos\,2\,\hat{\omega}\sigma_2 + \Xi_{14}\,sin\,2\,\hat{\omega}\sigma_2 = -{\mathrm{B}_1}^R, \\ \Xi_{21}\,cos\,\hat{\omega}\,\sigma_2 + \Xi_{22}\,sin\,\hat{\omega}\,\sigma_2 + \Xi_{23}\,cos\,2\,\hat{\omega}\sigma_2 + \Xi_{24}\,sin\,2\,\hat{\omega}\sigma_2 = -{\mathrm{B}_1}^I, \\ \Xi_{31}\,cos\,\hat{\omega}\,\sigma_2 + \Xi_{32}\,sin\,\hat{\omega}\,\sigma_2 + \Xi_{33}\,cos\,2\,\hat{\omega}\sigma_2 + \Xi_{34}\,sin\,2\,\hat{\omega}\sigma_2 = -{\mathrm{B}_2}^R, \\ \Xi_{41}\,cos\,\hat{\omega}\,\sigma_2 + \Xi_{42}\,sin\,\hat{\omega}\,\sigma_2 + \Xi_{43}\,cos\,2\,\hat{\omega}\sigma_2 + \Xi_{44}\,sin\,2\,\hat{\omega}\sigma_2 = -{\mathrm{B}_2}^I, \end{cases} \tag{19}$$

here

$$\begin{cases} \Xi_{11} = {\mathrm{B}_0}^R + {\mathrm{B}_2}^R, \quad \Xi_{12} = {\mathrm{B}_2}^I - {\mathrm{B}_0}^I, \quad \Xi_{13} = {\mathrm{B}_3}^R, \quad \Xi_{14} = {\mathrm{B}_3}^I, \\ \Xi_{21} = {\mathrm{B}_2}^I + {\mathrm{B}_0}^I, \quad \Xi_{22} = {\mathrm{B}_0}^R - {\mathrm{B}_2}^R, \quad \Xi_{23} = {\mathrm{B}_3}^I, \quad \Xi_{24} = -{\mathrm{B}_3}^R, \\ \Xi_{31} = {\mathrm{B}_1}^R + {\mathrm{B}_3}^R, \quad \Xi_{32} = {\mathrm{B}_3}^I - {\mathrm{B}_1}^I, \quad \Xi_{33} = {\mathrm{B}_0}^R, \quad \Xi_{34} = -{\mathrm{B}_0}^I, \\ \Xi_{41} = {\mathrm{B}_3}^I + {\mathrm{B}_1}^I, \quad \Xi_{42} = {\mathrm{B}_1}^R - {\mathrm{B}_3}^R, \quad \Xi_{43} = {\mathrm{B}_0}^I, \quad \Xi_{44} = {\mathrm{B}_0}^R. \end{cases}$$

Determinant of coefficient of equations (19)

$$\Xi = \begin{vmatrix} \Xi_{11} & \Xi_{12} & \Xi_{13} & \Xi_{14} \\ \Xi_{21} & \Xi_{22} & \Xi_{23} & \Xi_{24} \\ \Xi_{31} & \Xi_{32} & \Xi_{33} & \Xi_{34} \\ \Xi_{41} & \Xi_{42} & \Xi_{43} & \Xi_{44} \end{vmatrix}.$$

To ensure the existence of a unique solution to the system of equations, it is desirable that the coefficient matrix of equations (19) be non-singular.

Same as situation 2, using Cramer's law

$$\begin{cases} cos\,\hat{\omega}\,\sigma_2 = \frac{\Xi_1}{\Xi} = \hat{\Psi}_1(\hat{\omega}), \\ sin\,\hat{\omega}\,\sigma_2 = \frac{\Xi_2}{\Xi} = \hat{\Psi}_2(\hat{\omega}), \end{cases} \tag{20}$$

where

$$\Xi_1 = \begin{vmatrix} -\mathrm{B}_1^R & \Xi_{12} & \Xi_{13} & \Xi_{14} \\ -\mathrm{B}_1^I & \Xi_{22} & \Xi_{23} & \Xi_{24} \\ -\mathrm{B}_2^R & \Xi_{32} & \Xi_{33} & \Xi_{34} \\ -\mathrm{B}_2^I & \Xi_{42} & \Xi_{43} & \Xi_{44} \end{vmatrix}, \quad \Xi_2 = \begin{vmatrix} \Xi_{11} & -\mathrm{B}_1^R & \Xi_{13} & \Xi_{14} \\ \Xi_{21} & -\mathrm{B}_1^I & \Xi_{23} & \Xi_{24} \\ \Xi_{31} & -\mathrm{B}_2^R & \Xi_{33} & \Xi_{34} \\ \Xi_{41} & -\mathrm{B}_2^I & \Xi_{43} & \Xi_{44} \end{vmatrix}$$

From equations (20)

$${\hat{\Psi}_1}^2(\hat{\omega}) + {\hat{\Psi}_2}^2(\hat{\omega}) = 1. \tag{21}$$

Hypothesis 4 Equation (21) has positive real roots.

It follows from the first equation of equations (20) that

$$\widehat{\sigma_{2k}} = \frac{1}{\widehat{\omega}}[arccos(\widehat{\Psi}_1(\widehat{\omega}) + 2k\pi], = 0,1,2,\cdots \tag{22}$$

Define the first bifurcation point $\widehat{\sigma_{20}} = min\{\widehat{\sigma_{20}}, \cdots, \widehat{\sigma_{2k}}, \cdots\} = \frac{1}{\widehat{\omega}} arccos(\widehat{\Psi}_1(\widehat{\omega}))$ of the system (16).

Situation 4 $\sigma_3 > 0, \sigma_1 = \sigma_2 = 0$

Provided that $\sigma_3 > 0$,while $\sigma_1 = \sigma_2 = 0$, system (6) is transformed into the single delay system (23) as follows

$$\begin{cases} D^{\gamma_1} y_1(t) = -p_1 y_1(t) + \ell_1 y_1(t) + \wp_1 y_2(t) + x_1 y_3(t - \sigma_3), \\ D^{\gamma_2} y_2(t) = -p_2 y_2(t) + \ell_2 y_2(t) + \wp_2 y_3(t) + x_2 y_1(t - \sigma_3), \\ D^{\gamma_3} y_3(t) = -p_3 y_3(t) + \ell_3 y_3(t) + \wp_3 y_1(t) + x_3 y_2(t - \sigma_3), \end{cases}$$

the identity matrix of single time delay system (23) is:

$$\begin{pmatrix} s^{\gamma_1} + p_1 - \ell_1 & -\wp_1 & -x_1 e^{-s\sigma_3} \\ -x_2 e^{-s\sigma_3} & s^{\gamma_2} + p_2 - \ell_2 & -\wp_2 \\ -\wp_3 & -x_3 e^{-s\sigma_3} & s^{\gamma_3} + p_3 - \ell_3 \end{pmatrix}.$$

The characteristic equation of the system (23) is

$$\mathrm{C}_0(s) + \mathrm{C}_1(s) e^{-s\sigma_3} + \mathrm{C}_2(s) e^{-2s\sigma_3} + \mathrm{C}_3(s) e^{-3s\sigma_3} = 0, \tag{24}$$

where

$$\mathrm{C}_0(s) = s^{\gamma_1+\gamma_2+\gamma_3} + (p_3 - \ell_3) s^{\gamma_1+\gamma_2} + (p_2 - \ell_2) s^{\gamma_1+\gamma_3}$$

$$+(p_1 - \ell_1) s^{\gamma_2+\gamma_3} + (p_2 p_3 - p_2 \ell_3 - \ell_2 p_3 + \ell_2 \ell_3) s^{\gamma_1}$$

$$+(p_1 p_3 - p_1 \ell_3 - p_3 \ell_1 + \ell_1 \ell_3) s^{\gamma_2} + (p_1 p_2 - p_1 \ell_2 - p_2 \ell_1 + \ell_1 \ell_2) s^{\gamma_3}$$

$$+p_1 p_2 p_3 - p_1 p_2 \ell_3 - p_1 p_3 \ell_2 + p_1 \ell_2 \ell_3$$

$$-p_2 p_3 \ell_1 + p_2 \ell_1 \ell_3 + p_3 \ell_1 \ell_2 - \ell_1 \ell_2 \ell_3 - \wp_1 \wp_2 \wp_3$$

$$\mathrm{C}_1(s) = -\wp_3 x_1 (s^{\gamma_2} + p_2 - \ell_2) - \wp_1 x_2 (s^{\gamma_3} + p_3 - \ell_3)$$

$$-\wp_2 x_3 (s^{\gamma_1} + p_1 - \ell_1)$$

$$\mathrm{C}_2(s) = 0$$

$$\mathrm{C}_3(s) = -x_1 x_2 x_3$$

Multiplying $e^{s\sigma_3}$ and $e^{2s\sigma_3}$ on both sides of equation (24) directly yields the following equation

$$\begin{cases} \mathrm{C}_0(s) e^{s\sigma_3} + \mathrm{C}_1(s) + \mathrm{C}_2(s) e^{-s\sigma_3} + \mathrm{C}_3(s) e^{-2s\sigma_3} = 0, \\ \mathrm{C}_0(s) e^{2s\sigma_3} + \mathrm{C}_1(s) e^{s\sigma_3} + \mathrm{C}_2(s) + \mathrm{C}_3(s) e^{-s\sigma_3} = 0. \end{cases} \tag{25}$$

Let $s = \widetilde{\omega}(cos\frac{\pi}{2} + i\, sin\frac{\pi}{2})$, $\widetilde{\omega} > 0$ be the positive imaginary solution to the system of equations (25). For simplicity, we denote the real and imaginary parts of $C_i(s)$ $(i = 0,1,2,3)$ by $C_i^R(s)$ and $C_i^I(s)$, respectively.

$$\begin{cases} \mathrm{F}_{11}\cos(\tilde{\omega}\sigma_3)+\mathrm{F}_{12}\sin(\tilde{\omega}\sigma_3)+\mathrm{F}_{13}\cos(2\tilde{\omega}\sigma_3)+\mathrm{F}_{14}\sin(2\tilde{\omega}\sigma_3)=-\mathrm{C}_1^R, \\ \mathrm{F}_{21}\cos(\tilde{\omega}\sigma_3)+\mathrm{F}_{22}\sin(\hat{\omega}\sigma_3)+\mathrm{F}_{23}\cos(2\tilde{\omega}\sigma_3)+\mathrm{F}_{24}\sin(2\tilde{\omega}\sigma_3)=-\mathrm{C}_1^I, \\ \mathrm{F}_{31}\cos(\tilde{\omega}\sigma_3)+\mathrm{F}_{32}\sin(\hat{\omega}\sigma_3)+\mathrm{F}_{33}\cos(2\tilde{\omega}\sigma_3)+\mathrm{F}_{34}\sin(2\tilde{\omega}\sigma_3)=-\mathrm{C}_2^R, \\ \mathrm{F}_{41}\cos(\tilde{\omega}\sigma_3)+\mathrm{F}_{42}\sin(\tilde{\omega}\sigma_3)+\mathrm{F}_{43}\cos(2\tilde{\omega}\sigma_3)+\mathrm{F}_{44}\sin(2\tilde{\omega}\sigma_3)=-\mathrm{C}_2^I. \end{cases} \tag{26}$$

in here

$$\begin{cases} \mathrm{F}_{11}=\mathrm{C}_0{}^R+\mathrm{C}_2{}^R,\ \ \mathrm{F}_{12}=\mathrm{C}_2{}^I-\mathrm{C}_0{}^I,\ \ \mathrm{F}_{13}=\mathrm{C}_3{}^R,\ \ \mathrm{F}_{14}=\mathrm{C}_3{}^I, \\ \mathrm{F}_{21}=\mathrm{C}_0{}^I+\mathrm{C}_2{}^I,\ \ \mathrm{F}_{22}=\mathrm{C}_0{}^R-\mathrm{C}_2{}^R,\ \ \mathrm{F}_{23}=\mathrm{C}_3{}^I,\ \ \mathrm{F}_{24}=-\mathrm{C}_3{}^R, \\ \mathrm{F}_{31}=\mathrm{C}_1{}^R+\mathrm{C}_3{}^R,\ \ \ \mathrm{F}_{32}=\mathrm{C}_3{}^I-\mathrm{C}_1{}^I,\ \mathrm{F}_{33}=\mathrm{C}_0{}^R,\ \ \mathrm{F}_{34}=-\mathrm{C}_0{}^I, \\ \mathrm{F}_{41}=\ \mathrm{C}_1{}^I+\mathrm{C}_3{}^I,\ \ \mathrm{F}_{42}=\mathrm{C}_1{}^R-\mathrm{C}_3{}^R,\ \ \mathrm{F}_{43}=\mathrm{C}_0{}^I,\ \ \mathrm{F}_{44}=\mathrm{C}_0{}^R. \end{cases}$$

determinant of coefficient of equations (26)

$$\mathrm{F}=\begin{vmatrix} \mathrm{F}_{11} & \mathrm{F}_{12} & \mathrm{F}_{13} & \mathrm{F}_{14} \\ \mathrm{F}_{21} & \mathrm{F}_{22} & \mathrm{F}_{23} & \mathrm{F}_{24} \\ \mathrm{F}_{31} & \mathrm{F}_{32} & \mathrm{F}_{33} & \mathrm{F}_{34} \\ \mathrm{F}_{41} & \mathrm{F}_{42} & \mathrm{F}_{43} & \mathrm{F}_{44} \end{vmatrix}.$$

The existence of a unique solution to the system of equations requires that the coefficient matrix in equations (26) be non-singular.

Note 1 F_1, F_2expressions such as Ξ_1,Ξ_2 use Cramer's rule

$$\begin{cases} \cos\tilde{\omega}\,\sigma_3=\frac{\mathrm{F}_1}{\mathrm{F}}=\tilde{\Psi}_1(\tilde{\omega}), \\ \sin\tilde{\omega}\,\sigma_3=\frac{\mathrm{F}_2}{\mathrm{F}}=\tilde{\Psi}_2(\tilde{\omega}), \end{cases} \tag{27}$$

from the system of equations (27)

$$\tilde{\Psi}_1{}^2(\tilde{\omega})+\tilde{\Psi}_2{}^2(\tilde{\omega})=1. \tag{28}$$

Hypothesis 5 equation (28) has positive real roots

From (27)

$$\widetilde{\sigma_{3k}}=\frac{1}{\tilde{\omega}}\left[\arccos(\tilde{\Psi}_1(\tilde{\omega}))+2k\pi\right],\qquad k=0,1,2,\ldots \tag{29}$$

Define the first bifurcation point of the system (23), $\widetilde{\sigma_{30}}=min\{\widetilde{\sigma_{30}},\widetilde{\sigma_{31}},\cdots,\widetilde{\sigma_{3k}},\cdots\}=\frac{1}{\tilde{\omega}}arccos(\tilde{\Psi}_1(\tilde{\omega}))$.

The determination of the stability range for this situation is similar to the steps in Situation 2 and is omitted here.

Situation 5$\sigma_1\geq 0$, $\sigma_2\in(0,\widetilde{\sigma_{20}})$, $\sigma_3\in(0,\widetilde{\sigma_{30}})$

It should be noted that the connectivity adopted in this work is not arbitrarily constructed; rather, it is based on the prototypical structure of a three-neuron Hopfield network. In practical neural communication networks, both local feedback pathways and pathways originating from different sources often involve distinct transmission delays. Consequently, a topology composed of a self-connection delay plus two communication delays is reasonable. In this topology, σ_1 represents the intrinsic membrane delay arising from the neuron's self-regulatory inhibitory mechanism, whereas σ_2 and σ_3 correspond to delays associated with signals originating from different sources and

traveling along two communication routes of potentially different distances or media, whose transmission characteristics and temporal scales are often inconsistent.

Moreover, a three-node network constitutes the minimal structure capable of exhibiting multi-delay coupling effects, encompassing both local feedback and asymmetric coupling. This structure has thus been widely employed in studies of the stability and bifurcation mechanisms of delayed neural networks. The primary purpose of selecting this model is to investigate the cooperative effects among these three types of delays and to examine their impact on system stability, rather than to replicate a specific biological network. Furthermore, it has been shown that in three-node networks, differences in connection delays can significantly influence information transmission efficiency and overall network functioning; for instance, such effects have been observed in cortico-thalamo-cortical circuits [49].

When $\sigma_1 \geq 0$, $\sigma_2 \in (0, \widehat{\sigma_{20}})$, $\sigma_3 \in (0, \widetilde{\sigma_{3k}})$, and $\sigma_2 \neq \sigma_3$, σ_1 is treated as a bifurcation parameter in the analysis of bifurcation in system (6).

The identity matrix associated with the linear system (6) is given by:

$$\begin{pmatrix} s^{\gamma_1} + p_1 - \ell_1 e^{-s\sigma_1} & -\wp_1 e^{-s\sigma_2} & -x_1 e^{-s\sigma_3} \\ -x_2 e^{-s\sigma_3} & s^{\gamma_2} + p_2 - \ell_2 e^{-s\sigma_1} & -\wp_2 e^{-s\sigma_2} \\ -\wp_3 e^{-s\sigma_2} & -x_3 e^{-s\sigma_3} & s^{\gamma_3} + p_3 - \ell_3 e^{-s\sigma_1} \end{pmatrix}.$$

The characteristic equation of linear system (6) is

$$\mathrm{D}_0(s) + \mathrm{D}_1(s)e^{-s\sigma_1} + \mathrm{D}_2(s)e^{-2s\sigma_1} + \mathrm{D}_3(s)e^{-3s\sigma_1} = 0, \tag{30}$$

where

$$\begin{aligned}
\mathrm{D}_0(s) = {} & s^{\gamma_1+\gamma_2+\gamma_3} + p_3 s^{\gamma_1+\gamma_2} + p_2 s^{\gamma_1+\gamma_3} + p_1 s^{\gamma_2+\gamma_3} \\
& + p_2 p_3 s^{\gamma_1} + p_1 p_3 s^{\gamma_2} + p_1 p_2 s^{\gamma_3} + p_1 p_2 p_3 \\
& - \wp_1 \wp_2 \wp_3 e^{-3s\sigma_2} - x_1 x_2 x_3 e^{-3s\sigma_3} \\
& - (\wp_3 x_1 s^{\gamma_2} + \wp_3 p_2 x_1) e^{-s(\sigma_2+\sigma_3)} \\
& - (\wp_1 x_2 s^{\gamma_3} + \wp_1 p_3 x_2) e^{-s(\sigma_2+\sigma_3)} \\
& - (\wp_2 x_3 s^{\gamma_1} + \wp_2 p_1 x_3) e^{-s(\sigma_2+\sigma_3)}, \\
\mathrm{D}_1(s) = {} & -\ell_3 s^{\gamma_1+\gamma_2} - \ell_2 s^{\gamma_1+\gamma_3} - \ell_1 s^{\gamma_2+\gamma_3} \\
& - (p_2 \ell_3 + p_3 \ell_2) s^{\gamma_1} - (p_1 \ell_3 + p_3 \ell_1) s^{\gamma_2} \\
& - (p_1 \ell_2 + p_2 \ell_1) s^{\gamma_3} - p_1 p_3 \ell_2 - p_2 p_3 \ell_1 - p_1 p_2 \ell_3 \\
& + (\wp_3 \ell_2 x_1 + \wp_1 \ell_3 x_2 + \wp_2 \ell_1 x_3) e^{-s(\sigma_2+\sigma_3)}, \\
\mathrm{D}_2(s) = {} & \ell_1 \ell_2 s^{\gamma_3} + \ell_1 \ell_3 s^{\gamma_2} + \ell_2 \ell_3 s^{\gamma_1} \\
& + p_1 \ell_2 \ell_3 + p_2 \ell_1 \ell_3 + p_3 \ell_1 \ell_2, \\
\mathrm{D}_3(s) = {} & -\ell_1 \ell_2 \ell_3.
\end{aligned}$$

Multiplying $e^{s\sigma_1}$ and $e^{2s\sigma_1}$ on both sides of equation (30), we get

$$\begin{cases} \mathrm{D}_0(s)e^{s\sigma_1} + \mathrm{D}_1(s) + \mathrm{D}_2(s)e^{-s\sigma_1} + \mathrm{D}_3(s)e^{-2s\sigma_1} = 0, \\ \mathrm{D}_0(s)e^{2s\sigma_1} + \mathrm{D}_1(s)e^{s\sigma_1} + \mathrm{D}_2(s) + \mathrm{D}_3(s)e^{-s\sigma_1} = 0. \end{cases} \tag{31}$$

Let $s = \omega(cos\frac{\pi}{2} + i\, sin\frac{\pi}{2})(\omega > 0)$ be a positive imaginary root of equations (31), and ${D_i}^R$ and ${D_i}^I$ be the real and virtual parts of $D_i(s)(i = 0,1,2,3)$, respectively.

Now, separate the real part and virtual part

$$\begin{cases} \mathrm{P}_{11}\, cos\, \omega\, \sigma_1 + \mathrm{P}_{12}\, sin\, \omega\, \sigma_1 + \mathrm{P}_{13}\, cos\, 2\, \omega\sigma_1 + \mathrm{P}_{14}\, sin\, 2\, \omega\sigma_1 = -{\mathrm{D}_1}^R, \\ \mathrm{P}_{21}\, cos\, \omega\, \sigma_1 + \mathrm{P}_{22}\, sin\, \omega\, \sigma_1 + \mathrm{P}_{23}\, cos\, 2\, \omega\sigma_1 + \mathrm{P}_{24}\, sin\, 2\, \omega\sigma_1 = -{\mathrm{D}_1}^I, \\ \mathrm{P}_{31}\, cos\, \omega\, \sigma_1 + \mathrm{P}_{32}\, sin\, \omega\, \sigma_1 + \mathrm{P}_{33}\, cos\, 2\, \omega\sigma_1 + \mathrm{P}_{34}\, sin\, 2\, \omega\sigma_1 = -{\mathrm{D}_2}^R, \\ \mathrm{P}_{41}\, cos\, \omega\, \sigma_1 + \mathrm{P}_{42}\, sin\, \omega\, \sigma_1 + \mathrm{P}_{43}\, cos\, 2\, \omega\sigma_1 + \mathrm{P}_{44}\, sin\, 2\, \omega\sigma_1 = -{\mathrm{D}_2}^I, \end{cases} \tag{32}$$

here

$$\begin{cases} \mathrm{P}_{11} = {\mathrm{D}_0}^R + {\mathrm{D}_2}^R, \quad \mathrm{P}_{12} = {\mathrm{D}_2}^I - {\mathrm{D}_0}^I, \quad \mathrm{P}_{13} = {\mathrm{D}_3}^R, \quad \mathrm{P}_{14} = {\mathrm{D}_3}^I, \\ \mathrm{P}_{21} = {\mathrm{D}_0}^I + {\mathrm{D}_2}^I, \quad \mathrm{P}_{22} = {\mathrm{D}_0}^R - {\mathrm{D}_2}^R, \quad \mathrm{P}_{23} = {\mathrm{D}_3}^I, \quad \mathrm{P}_{24} = -{\mathrm{D}_3}^R, \\ \mathrm{P}_{31} = {\mathrm{D}_1}^R + {\mathrm{D}_3}^R, \quad \mathrm{P}_{32} = {\mathrm{D}_3}^I - {\mathrm{D}_1}^I, \quad \mathrm{P}_{33} = {\mathrm{D}_0}^R, \quad \mathrm{P}_{34} = -{\mathrm{D}_0}^I, \\ \mathrm{P}_{41} = {\mathrm{D}_1}^I + {\mathrm{D}_3}^I, \quad \mathrm{P}_{42} = {\mathrm{D}_1}^R - {\mathrm{D}_3}^R, \quad \mathrm{P}_{43} = {\mathrm{D}_0}^I, \quad \mathrm{P}_{44} = {\mathrm{D}_0}^R. \end{cases}$$

The characteristic equation of this part contains coefficients $D_0, D_1, D_2, D_3, \ldots$, but these coefficients themselves include exponential terms related to other time delays. The computation is large, and we will perform numerical solutions in Numerical simulations.

In order to verify Hopf's bifurcation condition, the following hypothesis is proposed in this paper.

Hypothesis 7 $\frac{\mathrm{G}_1\chi_1+\mathrm{G}_2\chi_2}{{\chi_1}^2+{\chi_2}^2} \neq 0$, where G_1, χ_1, G_2, χ_2 is described by equation (37).

Lemma 4 Let $s(\sigma_1) = \mu(\sigma_1) + i\omega(\sigma_1)$ be a solution of equation (30) satisfying $\mu({\sigma_1}^*) = 0$, $\omega({\sigma_1}^*) = \omega_0$ near $\sigma_1 = {\sigma_1}^*$. Then the following transversality condition holds

$$Re\left[\frac{ds}{d\sigma_1}\right]\Big|_{(\omega=\omega_0,\sigma_1={\sigma_1}^*)} \neq 0$$

Proof

The real and imaginary parts of ${D_i}'(s)$ can be expressed in terms of ${D_i}'^R$ and ${D_i}'^I$. According to the implicit function theorem, find the derivative of equation (30) with respect to σ_1

$$\frac{ds}{d\sigma_1} = \frac{\mathrm{G}(s)}{\chi(s)} = -\frac{F_{\sigma_1}}{F_s}, \tag{33}$$

of these,

$$\begin{aligned} F(\sigma_1, s) &= \mathrm{D}_0(s) + \mathrm{D}_1(s)e^{-s\sigma_1} + \mathrm{D}_2(s)e^{-2s\sigma_1} + \mathrm{D}_3(s)e^{-3s\sigma_1}, \\ \mathrm{G}(s) &= s[\mathrm{D}_1(s)e^{-s\sigma_1} + 2\mathrm{D}_2(s)e^{-2s\sigma_1} + 3\mathrm{D}_3(s)e^{-3s\sigma_1}], \\ \chi(s) &= {\mathrm{D}_0}'(s) + [{\mathrm{D}_1}'(s) - \sigma_1\mathrm{D}_1(s)]e^{-s\sigma_1} \\ &\quad + [{\mathrm{D}_2}'(s) - 2\sigma_1\mathrm{D}_2(s)]e^{-2s\sigma_1} \\ &\quad + [{\mathrm{D}_3}'(s) - 3\sigma_1\mathrm{D}_3(s)]e^{-3s\sigma_1}. \end{aligned}$$

From equation (37) it can be deduced that

$$Re\left[\frac{ds}{d\sigma_1}\right](\omega = \omega_0, \sigma_1 = {\sigma_1}^*) = \frac{G_1X_1 + G_2X_2}{{X_1}^2 + {X_2}^2}$$

$$
\begin{aligned}
G_1 &= \omega_0(D_1{}^R \sin \omega_0 \sigma_1{}^* - D_1{}^I \cos \omega_0 \sigma_1{}^* + 2D_2{}^R \sin 2\omega_0\sigma_1{}^* \\
&\quad -2D_2{}^I \cos 2\omega_0\sigma_1{}^* + 3D_3{}^R \sin 3\omega_0\sigma_1{}^* - 3D_3{}^I \cos 3\omega_0\sigma_1{}^*), \\
G_2 &= \omega_0(D_1{}^R \cos \omega_0 \sigma_1{}^* + D_1{}^I \sin \omega_0 \sigma_1{}^* + 2D_2{}^R \cos 2\omega_0\sigma_1{}^* \\
&\quad +2D_2{}^I \sin 2\omega_0\sigma_1{}^* + 3D_3{}^R \cos 3\omega_0\sigma_1{}^* + 3D_3{}^R \sin 3\omega_0\sigma_1{}^*), \\
\chi_1 &= D_0'^R + (D_1'^R - \sigma_1^* D_1^R)\cos(\omega_0\sigma_1^*) - (D_1'^I - \sigma_1^* D_1^I)\sin(\omega_0\sigma_1^*) \\
&\quad +(D_2'^R - 2\sigma_1^* D_2^R)\cos(2\omega_0\sigma_1^*) - (D_2'^I - 2\sigma_1^* D_2^I)\sin(2\omega_0\sigma_1^*) \\
&\quad +(D_3'^R - 3\sigma_1^* D_3^R)\cos(3\omega_0\sigma_1^*) - (D_3'^I - 3\sigma_1^* D_3^I)\sin(3\omega_0\sigma_1^*), \\
\chi_2 &= D_0'^I + (D_1'^R - \sigma_1^* D_1^R)\sin(\omega_0\sigma_1^*) + (D_1'^I - \sigma_1^* D_1^I)\cos(\omega_0\sigma_1^*) \\
&\quad +(D_2'^R - 2\sigma_1^* D_2^R)\sin(2\omega_0\sigma_1^*) + (D_2'^I - 2\sigma_1^* D_2^I)\cos(2\omega_0\sigma_1^*) \\
&\quad +(D_3'^R - 3\sigma_1^* D_3^R)\sin(3\omega_0\sigma_1^*) + (D_3'^I - 3\sigma_1^* D_3^I)\cos(3\omega_0\sigma_1^*).
\end{aligned}
$$

By Hypothesis 7, the transversality condition holds, thus completing the proof of Lemma 4.

We similarly prove the bifurcation points where the other two time delays give rise to bifurcations about Lemma 3, and give the stability ranges corresponding to these two time delays. On this basis, the bifurcation point of the system about the last time delay when these two time delays are in the stability range is further proved using Lemma 4. From this, we derive the following theorems.

Theorem 1 If Hypotheses 1 to 7 hold, then the following results hold

(1) If $\sigma_2 \in [0, \widehat{\sigma_{20}}), \sigma_3 \in [0, \widetilde{\sigma_{30}}), \sigma_1 \in [0, \sigma_1{}^*)$, the zero equilibrium point of system (5) is asymptotically stable.

(2) If $\sigma_2 \in [0, \widehat{\sigma_{20}})$, $\sigma_3 \in [0, \widetilde{\sigma_{30}})$, and $\sigma_1 > \sigma_1{}^*$, the zero equilibrium point of system (5) is unstable, and system (5) undergoes a Hopf bifurcation at $\sigma_1 = \sigma_1{}^*$.

Similarly situation 5 leads to situation 6 which leads to Theorem 2, and situation 7 which leads to Theorem 3.

Theorem 2 Under satisfying all the hypotheses, the following result can be obtained

(3) If $\sigma_1 \in [0, \overline{\sigma_{10}}), \sigma_3 \in [0, \widetilde{\sigma_{30}})$, when $\sigma_2 \in [0, \sigma_2{}^*)$, the zero equilibrium point of system (5) is asymptotically stable.

(4) If $\sigma_1 \in [0, \overline{\sigma_{10}}), \sigma_3 \in [0, \widetilde{\sigma_{30}})$, when $\sigma_2 \in [\sigma_2{}^*, +\infty)$, the zero equilibrium point of system (5) is unstable and system (5) undergoes a Hopf bifurcation at $\sigma_2 = \sigma_2{}^*$.

Theorem 3 Under satisfying all the hypotheses, the following result can be obtained

(5) If $\sigma_1 \in [0, \overline{\sigma_{10}}), \sigma_2 \in [0, \widehat{\sigma_{20}})$, when $\sigma_3 \in [0, \sigma_3{}^*)$, the zero equilibrium point of system (5) is asymptotically stable.

(6) If $\sigma_1 \in [0, \overline{\sigma_{10}}), \sigma_2 \in [0, \widehat{\sigma_{20}})$, when $\sigma_3 \in [\sigma_3{}^*, +\infty)$, the zero equilibrium point of system (5) is unstable and system (5) undergoes a Hopf bifurcation at $\sigma_3 = \sigma_3{}^*$.

5. Numerical Simulations

In order to verify the correctness of the results of the theoretical analysis in this paper, the system (4) is simulated numerically using the predictor-corrector scheme for systems of fractional order delay differential equations.

In the case of multiple discrete delays $\sigma_1, \sigma_2, \sigma_3$ that are not integer multiples of each other, the delayed terms $y(t-\sigma_j)$ generally do not fall on the computational grid points $t_k = kh$. In this work, we handle the delayed terms in the predictor–corrector method using linear interpolation. where t_m and t_{m+1} are the grid points satisfying $t_m \le t_k - \sigma_j \le t_{m+1}$. Where system (1) in $t \in [0, T]$, assume that t is divided into N,that is $\{t_n = nh : n = k+2, \cdots, N+k\}$ and satisfies $h = T/N$, $k = max[\frac{\sigma_1}{h}, \frac{\sigma_2}{h}, \frac{\sigma_3}{h}]$, where $y(t_j - \sigma_i) = y(jh - k_i h) = y(t_{j-k_i})$,$j \in Z$ and $k \le j \le n-2$. Denote $y_{n+1,i} = y_{i,n}(t_{n+1})$ as the approximate value of y_i at t_{n+1} in the system (5) using the predictor-corrector method,$i = 1,2,3$.

Firstly, according to (2), the system (5) is discretized and the discrete form is

$$\begin{aligned}
y_{n+1,1} = y_{0,1} + \frac{h^{\gamma_1}}{\gamma(\gamma_1+2)}[&-p_1 y_{n+1,1}^p \\
&+\iota_1 \tanh(y_{n+1-k_1,1}^p) + \rho_1 \tanh(y_{n+1-k_2,1}^p) \\
&+\kappa_1 \tanh(y_{n+1-k_3,1}^p) + \textstyle\sum_{j=0}^{n} a_{j,n+1}(-p_1 y_{j,1} \\
&+\iota_1 \tanh(y_{j-k_1,1}) + \rho_1 \tanh(y_{j-k_2,1}) \\
&+\kappa_1 \tanh(y_{j-k_3,1}))],
\end{aligned}$$

$$\begin{aligned}
y_{n+1,2} = y_{0,2} + \frac{h^{\gamma_2}}{\gamma(\gamma_2+2)}[&-p_2 y_{n+1,2}^p + \iota_2 \tanh(y_{n+1-k_1,2}^p) \\
&+\rho_2 \tanh(y_{n+1-k_2,2}^p) + \kappa_2 \tanh(y_{n+1-k_3,2}^p) \\
&+\textstyle\sum_{j=0}^{n} a_{j,n+1}(-p_2 y_{j,2} + \iota_2 \tanh(y_{j-k_1,2}) \\
&+\rho_2 \tanh(y_{j-k_2,2}) + \kappa_2 \tanh(y_{j-k_3,2}))],
\end{aligned}$$

$$\begin{aligned}
y_{n+1,3} = y_{0,3} + \frac{h^{\gamma_3}}{\gamma(\gamma_3+2)}[&-p_3 y_{n+1,3}^p + \iota_3 \tanh(y_{n+1-k_1,3}^p) \\
&+\rho_3 \tanh(y_{n+1-k_2,3}^p) + \kappa_3 \tanh(y_{n+1-k_3,3}^p) \\
&+\textstyle\sum_{j=0}^{n} a_{j,n+1}(-p_3 y_{j,3} + \iota_3 \tanh(y_{j-k_1,3}) \\
&+\rho_3 \tanh(y_{j-k_2,3}) + \kappa_3 \tanh(y_{j-k_3,3}))].
\end{aligned}$$

The following three examples are discussed for simulation experiments on system (5). The examples chosen in this paper have several significant advantages to fully reflect the complexity and representativeness of the system.

Firstly, in the choice of fractional order, we adopt three different orders, avoiding the monotonicity of the uniform order, making the model more suitable for the situation of inconsistent system memory effects in practice, and reflecting the flexibility and wide applicability of fractional order systems.

Second, in the design of coefficients, we especially chose the settings of mixed positive and negative coefficients with various size distributions, which not only reflects the real structure of the coexistence of excitation and inhibition among neural networks but also increases the nonlinear complexity of the system.

Third, in the initial value selection, we set all three initial values non-zero and different, which enhances the generality and persuasiveness of the system simulation. Finally, in the setting of time delay parameters, we demonstrate the effect on the other time delay and the stability and bifurcation behavior of the system by first introducing two different time delays and adjusting them within a certain range. In particular, in combination with the analysis of the change of the bifurcation point, we reveal the evolution mechanism of the system from stability to oscillation, highlighting the time delay sensitivity and regulation potential of fractional-order time delay neural networks.

In summary, good stabilization or bifurcation behaviors are still observed under different parameter settings.

5.1. Example 1

In this example, the bifurcation problem of system (34) is investigated by discussing situation $5\sigma_1 > 0, \sigma_2 \in (0, \widehat{\sigma_{20}})$, $\sigma_3 \in (0, \widetilde{\sigma_{30}})$ with σ_1 as the bifurcation parameter

$$\begin{cases}
D^{0.65} y_1(t) = -1.8 y_1(t) + 1.2 \tanh(y_1(t-\sigma_1)) \\
\qquad\qquad +2.1 \tanh(y_2(t-\sigma_2)) + 1.3 \tanh(y_3(t-\sigma_3)), \\
D^{0.67} y_2(t) = -1.1 y_2(t) + 1.2 \tanh(y_2(t-\sigma_1)) \\
\qquad\qquad -0.9 \tanh(y_3(t-\sigma_2)) - 1.3 \tanh(y_1(t-\sigma_3)), \\
D^{0.68} y_3(t) = -1.2 y_3(t) - 1.3 \tanh(y_3(t-\sigma_1)) \\
\qquad\qquad +0.9 \tanh(y_1(t-\sigma_2)) - 1.2 \tanh(y_2(t-\sigma_3)),
\end{cases} \tag{35}$$

In this system (39), The step size is $h = 0.1$, its initial conditions we can set as $(y_1(0), y_2(0), y_3(0)) = (0.01, -0.01, 0.01)$, $\sigma_2 = 0.6$, $\sigma_3 = 0.9$.

From the parameter settings, we know that the Hypotheses 1-7 are satisfied, and we can clearly figure out that $\omega = 0.4315$, according (30) ${\sigma_1}^* = 1.6301$, when $\sigma_1 = 1.62 < {\sigma_1}^*$, the zero equilibrium point of the system (32) is asymptotically stable, as shown in Fig. (**2**) knowing that (1) of Theorem 1 holds, when $\sigma_1 = 1.66 > {\sigma_1}^*$, the system loses its stability, and starts to oscillate, as shown in Fig. (**4**), and in Fig. (**5**), it is clearly and intuitively shown that when $\sigma_1 = {\sigma_1}^*$, the bifurcation occurs, So as in Fig. (**3**) and Fig. (**5**) it can be seen that (2) of Theorem 1 holds.

In Fig. (**6**), we can clearly see the effect of the time delays combination (σ_2, σ_3) on ${\sigma_1}^*$,when the communication delays σ_2 and σ_3 are both small (i.e., near the origin of the coordinate plane), the critical value ${\sigma_1}^*$ is correspondingly large. As σ_2 and σ_3 increase, the critical value${\sigma_1}^*$ decreases. This reveals a dynamic, mutually compensatory trade-off between the two delays. which also tells us that ${\sigma_1}^*$ is not only controlled by the parameter only; through Fig. (**7**), we can see that the stability interval of the fractional order neural network is longer than that of the integer order neural network, and the range of the adjustable time delay is wider in the stability interval.

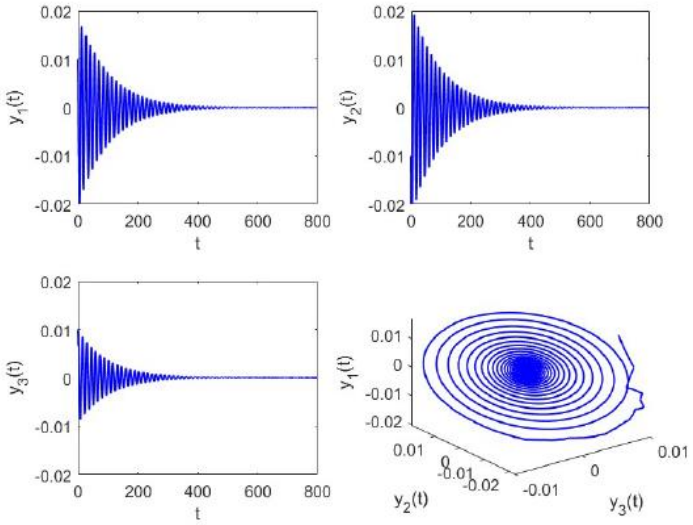

Figure 2: The time-series and phase diagrams of system (35), $\sigma_2 = 0.6$, $\sigma_3 = 0.9$, $\sigma_1 = 1.62 < {\sigma_1}^* = 1.6301$.

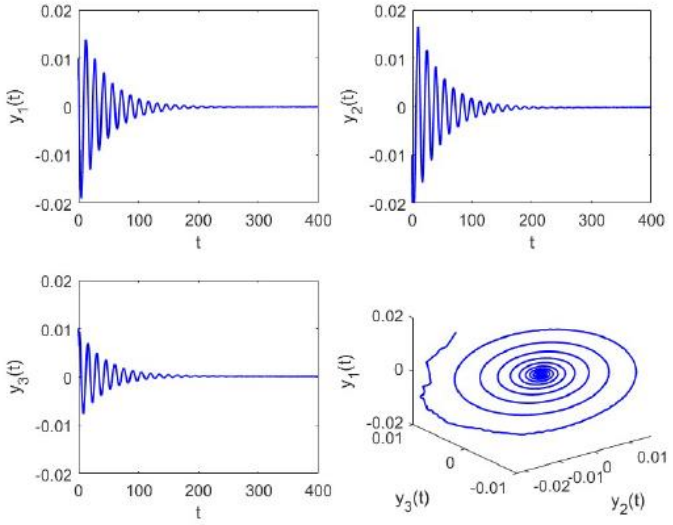

Figure 3: This set of figures shows three different orders $\gamma_1 = 0.5$, $\gamma_2 = 0.6$, $\gamma_3 = 0.7$. Compared with Example 1, although the orders are different, the resulting effects are similar and do not depend on a particular choice of the ending.

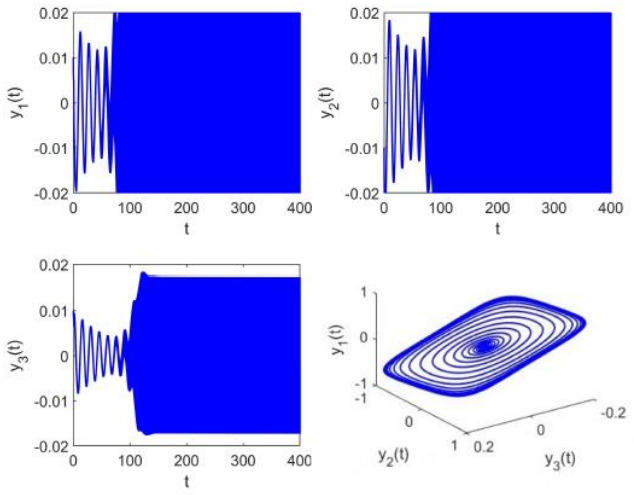

Figure 4: The time-series and phase diagrams of system (35),$\sigma_2 = 0.6$,$\sigma_3 = 0.9$,$\sigma_1 = 1.66 > \sigma_1^* = 1.6301$.

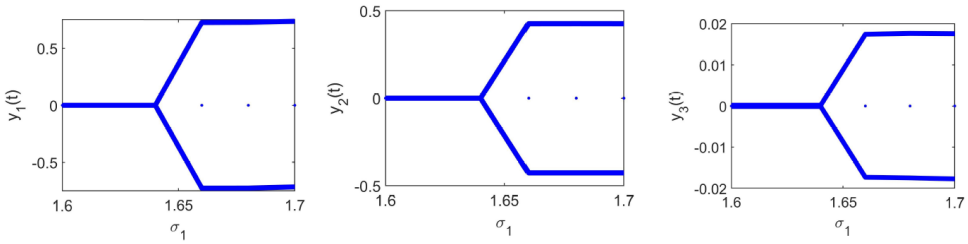

Figure 5: The system (35) bifurcation diagrams with respect to σ_1, $\sigma_2 = 0.6$, $\sigma_3 = 0.9$

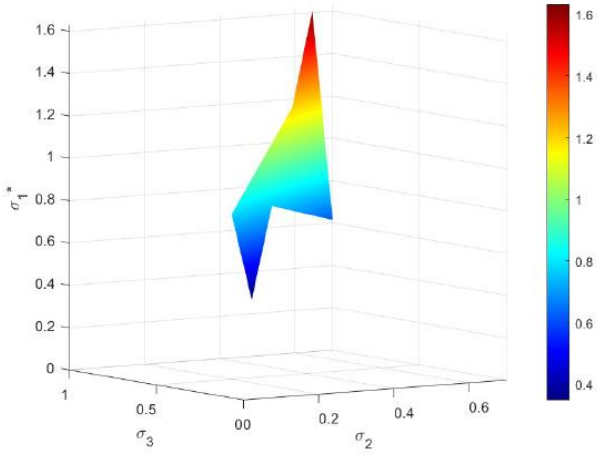

Figure 6: The three-dimensional plot of the effect of the combination of delays (σ_2, σ_3) on σ_1^* in system (39).

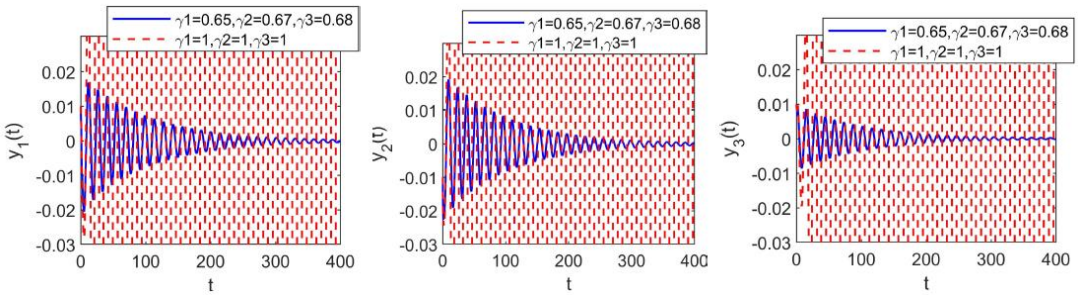

Figure 7: Comparison of the convergence of $\gamma_1 = 0.65, \gamma_2 = 0.67, \gamma_3 = 0.68$ with $\gamma_1 = 1, \gamma_2 = 1, \gamma_3 = 1$.

5.2. Example 2

In this example, situation 6 $\sigma_2 > 0$, $\sigma_1 \in (0, \overline{\sigma_{10}})$, $\sigma_3 \in (0, \widetilde{\sigma_{30}})$ are discussed to study the bifurcation of system (39) using σ_2 as the bifurcation parameter

$$\begin{cases} D^{0.94}y_1(t) &= 1.4y_1(t) + 0.9\,tanh(y_1(t-\sigma_1)) - 0.9\,tanh(y_2(t-\sigma_2)) \\ &\quad -1.3\,tanh(y_3(t-\sigma_3)), \\ D^{0.95}y_2(t) &= 1.1y_2(t) - 0.9\,tanh(y_2(t-\sigma_1)) + 0.9\,tanh(y_3(t-\sigma_2)) \\ &\quad -1.2\,tanh(y_1(t-\sigma_3)), \\ D^{0.98}y_3(t) &= 1.4y_3(t) - 1\,tanh(y_3(t-\sigma_1)) - 0.8\,tanh(y_1(t-\sigma_2)) \\ &\quad -1.9\,tanh(y_2(t-\sigma_3)), \end{cases} \tag{36}$$

In this system (36),The step size is $h = 0.05$, its initial conditions we can set as $(y_1(0), y_2(0), y_3(0)) = (0.05, 0.01, 0.02)$, $\sigma_1 = 0.6$, $\sigma_3 = 1.2$.

Because all the hypotheses are satisfied, we can clearly work out that $\omega = 0.6994$, since Situation 6 has been omitted, the calculation of σ_2^* is the same as that of σ_2^* to obtain $\sigma_2^* = 4.3255$, the zero equilibrium point of the system (36) is asymptotically stable when $\sigma_2 = 4.3 < \sigma_2^*$, Theorem 2 (3) holds as shown in Fig. (**8**), and the system loses its stability and starts to oscillate when $\sigma_2 = 4.8 > \sigma_2^*$, as shown in Fig. (**9**), and it is clearly and intuitively demonstrated that bifurcation occurs when $\sigma_2 = \sigma_2^*$ in Fig. (**10**), as in Fig. (**9**) and Fig. (**10**) know that Theorem 2 (4) holds.

In Fig. (**11**),as the self-connection delay σ_1 or the communication delay σ_3 increases, the critical delay σ_2^* exhibits a pronounced decreasing trend.The rates of change along the σ_1 axis and the σ_3 axis are found to be different. The surface may be steeper in the σ_1 direction than in the σ_3 direction. This indicates that, in this particular system, the critical communication delay σ_2^* is more sensitive to variations in the self-connection delay σ_1.

By comparing the convergence of the fractional order neural network and the integer order neural network in Fig. (**12**), we can see that the integer order neural network oscillates a little bit more obviously than the fractional order.

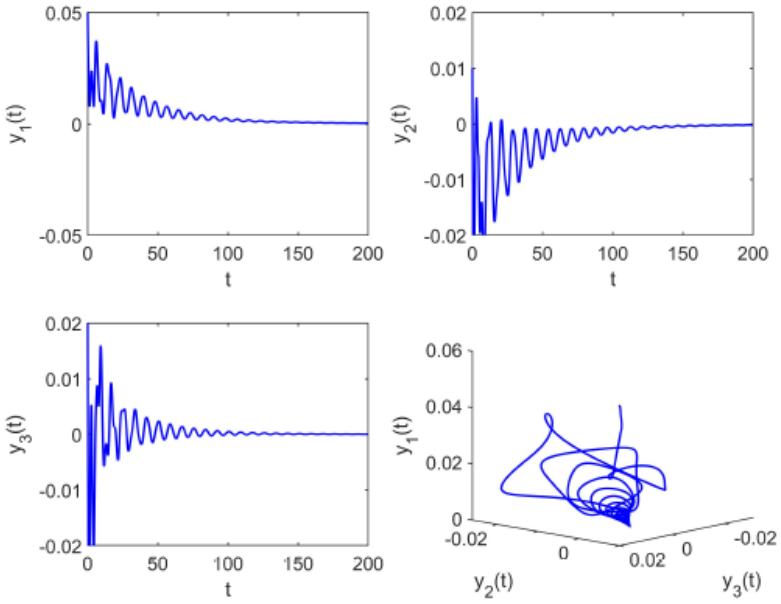

Figure 8: The time-series and phase diagrams of system (36),$\sigma_1 = 0.6$,$\sigma_3 = 1.2$,$\sigma_2 = 4.3 < \sigma_2^* = 4.3255$.

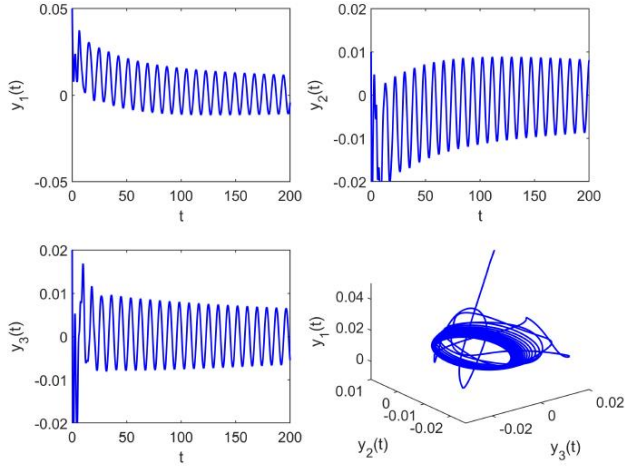

Figure 9: The time-series and phase diagrams of system (36),$\sigma_1 = 0.6,\sigma_3 = 1.2,\sigma_2 = 4.8 > \sigma_2^* = 4.3255$.

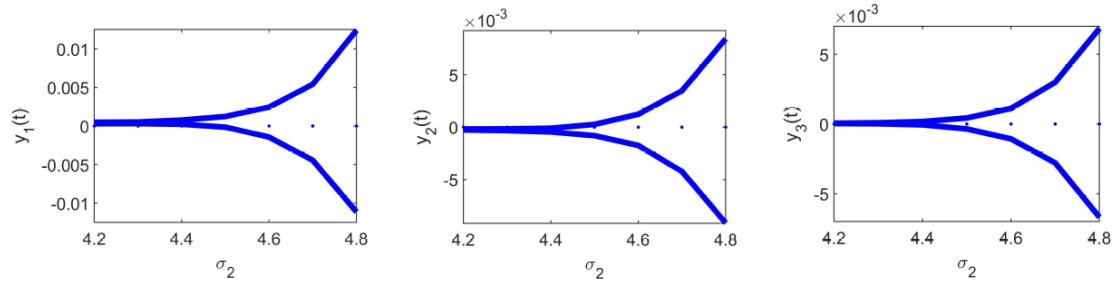

Figure 10: The system (36) bifurcation diagrams with respect to $\sigma_2,\sigma_1 = 0.6,\sigma_3 = 1.2$.

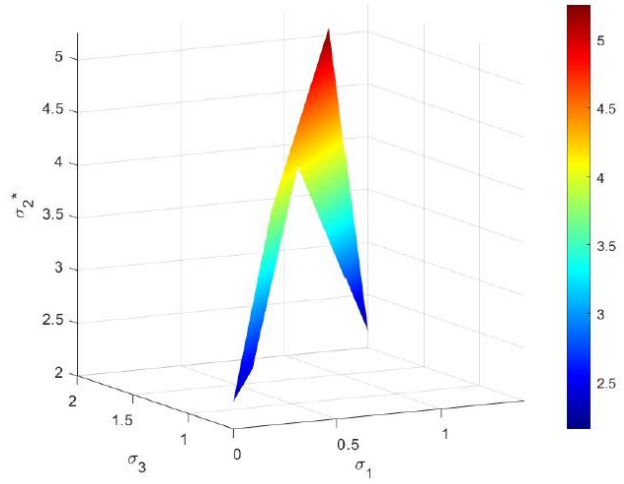

Figure 11: The three-dimensional plot of the effect of the combination of delays (σ_1, σ_3) on σ_2^* in system (36).

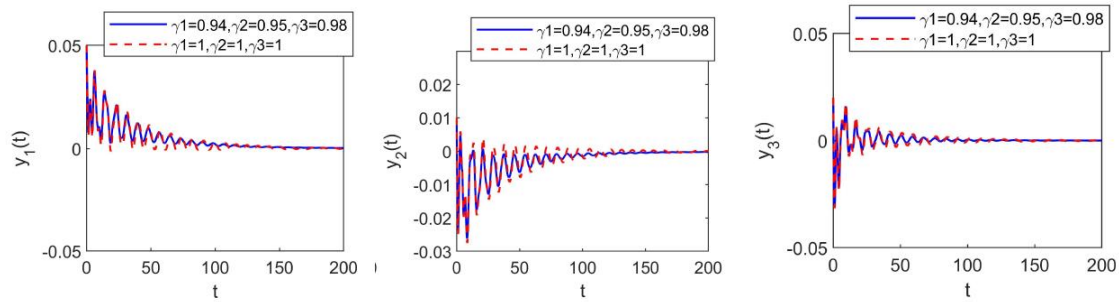

Figure 12: The comparison of the convergence of $\gamma_1 = 0.94, \gamma_2 = 0.95, \gamma_3 = 0.98$ with $\gamma_1 = 1, \gamma_2 = 1, \gamma_3 = 1$.

5.3. Example 3

In this example, situation $7\sigma_3 > 0$, $\sigma_1 \in (0, \overline{\sigma_{10}})$, $\sigma_2 \in (0, \widehat{\sigma_{20}})$ are discussed to study the bifurcation of system (36) with σ_3 as the bifurcation parameter

$$\begin{cases} D^{0.92}y_1(t) &= 0.5y_1(t) - 0.7\,tanh(\,y_1(t-\sigma_1)) - 1\,tanh(\,y_2(t-\sigma_2)) \\ &\quad -1.2\,tanh(\,y_3(t-\sigma_3)), \\ D^{0.91}y_2(t) &= 0.4y_2(t) - 0.5\,tanh(\,y_2(t-\sigma_1)) + 0.5\,tanh(\,y_3(t-\sigma_2)) \\ &\quad +1\,tanh(\,y_1(t-\sigma_3)), \\ D^{0.97}y_3(t) &= 0.6y_3(t) - 0.5\,tanh(\,y_3(t-\sigma_1)) - 0.8\,tanh(\,y_1(t-\sigma_2)) \\ &\quad -1\,tanh\,y_2\,(t-\sigma_3)), \end{cases} \tag{37}$$

In this system (37), whose initial conditions we can set as $(y_1(0), y_2(0), y_3(0)) = (0.03, -0.03, 0.03)$, $\sigma_1 = 1.8$, $\sigma_2 = 2.1$,$h = 0.1$.

From all the above hypotheses, we can clearly work out $\omega = 1.3695$,since Situation 7 has been omitted, the calculation of ${\sigma_3}^*$ is the same as that of ${\sigma_1}^*$ to obtain ${\sigma_3}^* = 0.4310$, when $\sigma_3 = 0.43 < {\sigma_3}^*$, the zero equilibrium point of the system (40) is asymptotically stable, Theorem 3(5) holds as seen in Fig. (**13**), when $\sigma_3 = 0.45 > {\sigma_3}^*$, the system loses its stability and starts to oscillate as shown in Fig. (**14**), and in Fig. (**15**) it is clearly visualised that the bifurcation occurs when $\sigma_3 = {\sigma_3}^*$, Thus from Fig. (**13**) and Fig. (**14**), Theorem 3(6) holds.

In Fig. (**16**) it can be clearly see the simultaneous increase of the self-connection delay σ_1 and the communication delay σ_2 can significantly suppress ${\sigma_3}^*$ and in this example we also compare the stability of the fractional order neural networks with that of the integer order neural network. It is clear that the stability and dynamic performance of the fractional order neural network is better in Fig. (**17**).

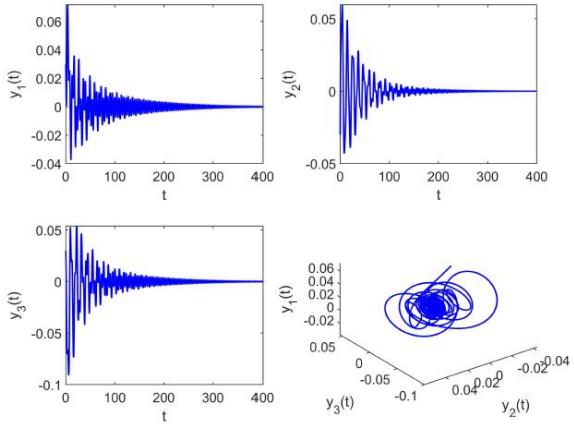

Figure 13: The time-series and phase diagrams of system (37), $\sigma_1 = 1.8$,$\sigma_2 = 2.1$,$\sigma_3 = 0.43 < {\sigma_3}^* = 0.4310$.

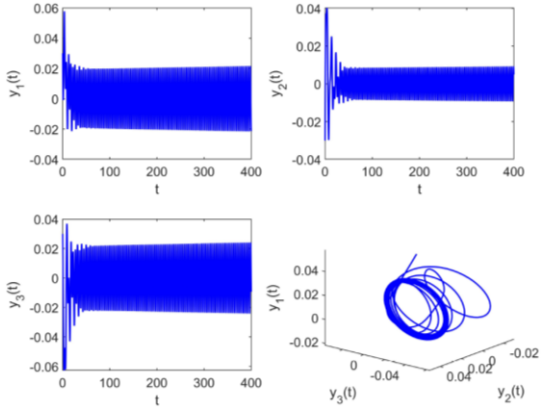

Figure 14: The time-series and phase diagrams of system (37), $\sigma_1 = 1.8$,$\sigma_2 = 2.1$,$\sigma_3 = 0.45 > {\sigma_3}^* = 0.4310$.

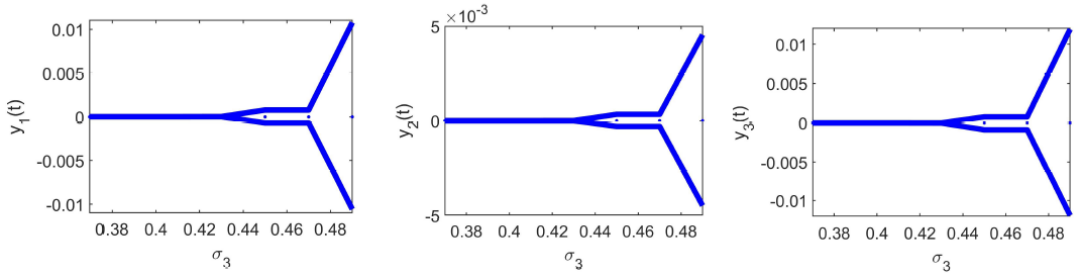

Figure 15: The system (37) bifurcation diagrams with respect to σ_3,$\sigma_1 = 1.8$,$\sigma_2 = 2.1$.

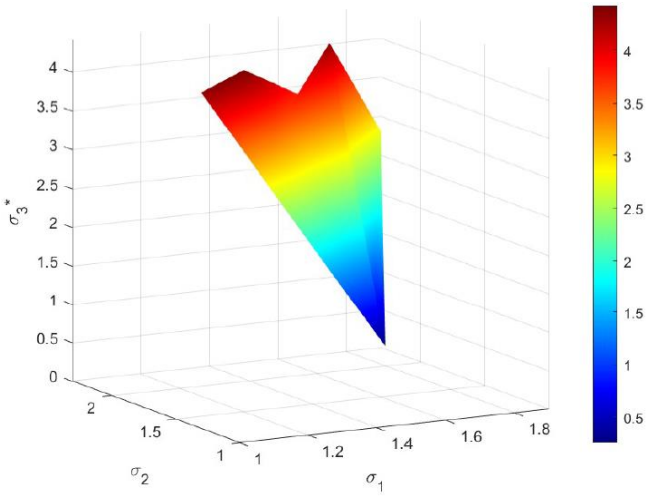

Figure 16: The three-dimensional plot of the effect of the combination of delays (σ_1, σ_2) on $\sigma_3{}^*$ in system (40).

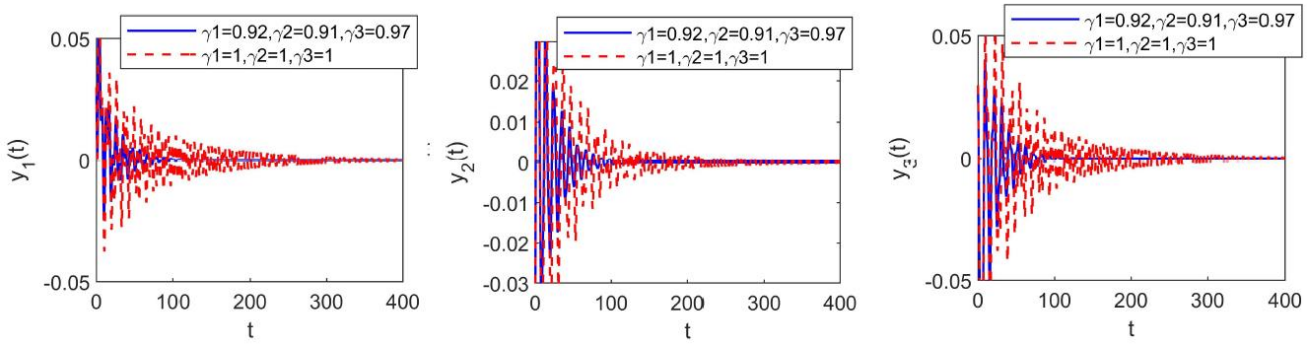

Figure 17: The comparison of the convergence of $\gamma_1 = 0.92, \gamma_2 = 0.91, \gamma_3 = 0.97$ with $\gamma_1 = 1, \gamma_2 = 1, \gamma_3 = 1$.

6. Conclusion

Delays are inherent in many real-world systems. In neuroscience, different types of delays directly affect the speed of information processing and cognitive functions; in communication networks, multi-delay factors determine the reliability, congestion level, and real-time performance of data transmission; in distributed control and robotic systems, mismatches between local and remote feedback delays may critically influence system stability and the success of cooperative tasks. Therefore, multi-delay effects are not merely theoretical constructs but fundamental factors shaping the behavior of biological and engineering networks.

In this paper, we established and analyzed a fractional-order Hopfield neural network with three distinct delays: one self-connection delay and two communication delays. Because these delays interact nonlinearly, conventional delay-transformation techniques cannot be applied directly. To overcome this difficulty, we derived the characteristic equation containing three transcendental terms and developed a general strategy to solve for the

bifurcation points by combining structural properties of the equation with Cramer's rule. On this basis, an explicit Hopf bifurcation criterion was obtained, allowing us to determine the stability region of the system.

The theoretical results demonstrate that when each delay remains below its critical value, the equilibrium point is asymptotically stable. Once any delay exceeds its threshold, the system undergoes Hopf bifurcation and transitions into periodic oscillations. Moreover, the coupling effects among the three delays significantly shift the bifurcation boundaries, indicating that system stability is jointly shaped by internal and communication delays rather than by a single delay parameter. Additionally, comparative analyses show that fractional-order neural networks possess larger stability regions and stronger oscillation-suppressing capabilities than their integer-order counterparts, confirming the beneficial role of fractional memory in delaying bifurcations and enhancing stability.

From a numerical perspective, we employed an improved predictor–corrector method tailored for fractional multi-delay systems. This approach effectively captures the nonlocal memory of fractional derivatives while maintaining high numerical accuracy and stability, making it a reliable computational tool for studying complex fractional-order neural dynamics. The numerical simulations agree closely with the theoretical predictions, further validating the correctness and robustness of the proposed analysis framework.

Beyond the specific model studied here, the analytical techniques and numerical methodology developed in this work have broad applicability. They can be extended to gene regulatory networks, multi-agent cooperative systems, neuromorphic circuits, and the stability analysis of modern power grids, where multiple types of delays and memory effects coexist. Therefore, this study not only advances the theoretical development of multi-delay fractional dynamical systems but also provides practical tools and insights for stability control, delay management, and performance optimization in complex networked systems.

Conflict of Interest

The authors declare that there are no conflicts of interest, including any financial or personal relationships that could have influenced the work reported in this paper.

Funding

This work was supported by a Ministry of Education Industry-University-Research Collaboration Project (Grant No. 2024H60057).

Acknowledgments

None.

Data Availability

The datasets used and/or analyzed during the current study are available from the corresponding author on reasonable request.

Authors' Contributions

All authors contributed equally to the study.

References

[1] Laskin N. Fractional quantum mechanics. Phys Rev E. 2000; 62(3): 3135. https://doi.org/10.1103/PhysRevE.62.3135

[2] Goufo EFD, Kumar S, Mugisha SB. Similarities in a fifth-order evolution equation with and with no singular kernel. Chaos Solitons Fractals. 2020; 130: 109467. https://doi.org/10.1016/j.chaos.2019.109467

[3] Tuan NH, Mohammadi H, Rezapour S. A mathematical model for COVID-19 transmission by using the Caputo fractional derivative. Chaos

Solitons Fractals. 2020; 140: 110107. https://doi.org/10.1016/j.chaos.2020.110107

[4] Koller RC. Applications of fractional calculus to the theory of viscoelasticity. J Appl Mech. 1984; 51(2): 299-307. https://doi.org/10.1115/1.3167616

[5] Smith H. An introduction to delay differential equations with applications to the life sciences. Germany: Springer; 2011.

[6] Lakshmanan M, Senthilkumar DV. Dynamics of nonlinear time-delay systems. Germany: Springer Science & Business Media; 2011. https://doi.org/10.1007/978-3-642-14938-2

[7] Lainscsek C, Rowat P, Schettino L, Lee D, Song D, Letellier C, et al. Finger tapping movements of Parkinson's disease patients automatically rated using nonlinear delay differential equations. Chaos. 2012; 22(1): 013119. https://doi.org/10.1063/1.3683444

[8] Lainscsek C, Sejnowski TJ. Electrocardiogram classification using delay differential equations. Chaos. 2013; 23(2): 023132. https://doi.org/10.1063/1.4811544

[9] Matigon D. Computational engineering in systems and application multiconference. IMACS, IEEE-SMC, France. 1996; 12: 963.

[10] Pakzad MA, Pakzad S. Stability map of fractional order time-delay systems. WSEAS Trans Syst. 2012; 10(11): 541-50.

[11] Bonnet C, Partington JR. Analysis of fractional delay systems of retarded and neutral type. Automatica. 2002; 38(7): 1133-8. https://doi.org/10.1016/S0005-1098(01)00306-5

[12] Hwang C, Cheng YC. A numerical algorithm for stability testing of fractional delay systems. Automatica. 2006; 42(5): 825-31. https://doi.org/10.1016/j.automatica.2006.01.008

[13] Bhalekar SB. Stability analysis of a class of fractional delay differential equations. Pramana. 2013; 81(2): 215-24. https://doi.org/10.1007/s12043-013-0569-5

[14] Bhalekar S. Stability and bifurcation analysis of a generalized scalar delay differential equation. Chaos. 2016; 26(8): 084306. https://doi.org/10.1063/1.4958923

[15] Bhalekar S, Daftardar-Gejji V. Synchronization of different fractional order chaotic systems using active control. Commun Nonlinear Sci Numer Simul. 2010; 15(11): 3536-46. https://doi.org/10.1016/j.cnsns.2009.12.016

[16] Daftardar-Gejji V, Bhalekar S, Gade P. Dynamics of fractional-ordered Chen system with delay. Pramana. 2012; 79: 61-9. https://doi.org/10.1007/s12043-012-0291-8

[17] Bhalekar S. Dynamical analysis of fractional order Uçar prototype delayed system. Signal Image Video Process. 2012; 6: 513-9. https://doi.org/10.1007/s11760-012-0330-4

[18] Bhalekar S, Daftardar-Gejji V, Baleanu D, Magin R. Fractional Bloch equation with delay. Comput Math Appl. 2011; 61(5): 1355-65. https://doi.org/10.1016/j.camwa.2010.12.079

[19] Bhalekar S, Daftardar-Gejji V, Baleanu D, Magin R. Generalized fractional order Bloch equation with extended delay. Int J Bifurc Chaos. 2012; 22(4): 1250071. https://doi.org/10.1142/S021812741250071X

[20] Shiri B, Shi YG, Baleanu D. The well-posedness of incommensurate FDEs in the space of continuous functions. Symmetry. 2024; 16(8): 1058. https://doi.org/10.3390/sym16081058

[21] Shiri B. Well-posedness of the mild solutions for incommensurate systems of delay fractional differential equations. Fractal Fract. 2025; 9(2): 60. https://doi.org/10.3390/fractalfract9020060

[22] Shiri B, Shi YG, Baleanu D. Hyers-Ulam stability of systems of incommensurate fractional differential equations. Authorea Preprints. 2024. https://doi.org/10.22541/au.172926371.14355260/v1

[23] Shiri B, Khiabani ED, Baleanu D. Analysis and analytical solution of incommensurate fuzzy fractional nabla difference systems in neural networks. Theor Appl. 2025; 15(4): 610-24. https://doi.org/10.36922/IJOCTA025130067

[24] Baleanu D, Shiri B. Generalized fractional differential equations for past dynamic. AIMS Math. 2022; 7(8): 14394-418. https://doi.org/10.3934/math.2022793

[25] Wang H, Yu Y, Wen G. Stability analysis of fractional-order Hopfield neural networks with time delays. Neural Netw. 2014; 55: 98. https://doi.org/10.1016/j.neunet.2014.03.012

[26] Yuan J, Huang C. Quantitative analysis in delayed fractional-order neural networks. Neural Process Lett. 2019; 50: 1631-51. https://doi.org/10.1007/s11063-019-10161-2

[27] Hale JK, Huang WZ. Global geometry of the stable regions for two delay differential equations. J Math Anal Appl. 1993; 178(2): 344-62. https://doi.org/10.1006/jmaa.1993.1312

[28] Bélair J, Campbell SA. Stability and bifurcations of equilibria in a multiple-delayed differential equation. SIAM J Appl Math. 1994; 54(5): 1402-24. https://doi.org/10.1137/S0036139993248853

[29] Li X, Ruan S, Wei J. Stability and bifurcation in delay-differential equations with two delays. J Math Anal Appl. 1999; 236(2): 254-80. https://doi.org/10.1006/jmaa.1999.6418

[30] Qie X, Zang J, Liu S, Shilnikov AL. Synaptic delays shape dynamics and function in multimodal neural motifs. Chaos. 2025; 35(4): 043106. https://doi.org/10.1063/5.0233640

[31] Tsianos KI, Rabbat MG. The impact of communication delays on distributed consensus algorithms. arXiv preprint arXiv:1207.5839. 2012.

[32] Zhao Y, Paine N, Kim KS, Sentis L. Stability and performance limits of latency-prone distributed feedback controllers. IEEE Trans Ind Electron. 2015; 62(11): 7151-62. https://doi.org/10.1109/TIE.2015.2448513

[33] Li B, Cheng X. Synchronization analysis of coupled fractional-order neural networks with time-varying delays. Math Biosci Eng. 2023; 20: 14846-65. https://doi.org/10.3934/mbe.2023665

[34] Ma Y, Lin Y, Dai Y. Stability and Hopf bifurcation analysis of a fractional-order BAM neural network with two delays under hybrid control. Neural Process Lett. 2024; 56(2): 82. https://doi.org/10.1007/s11063-024-11458-7

[35] Kumar P, Erturk VS, Murillo-Arcila M, Govindaraj V. A new form of L1-predictor-corrector scheme to solve multiple delay-type fractional order systems with the example of a neural network model. Fractals. 2023; 31(4): 2340043. https://doi.org/10.1142/S0218348X23400431

[36] Sivalingam SM, Kumar P, Trinh H, Govindaraj V. A novel L1-Predictor-Corrector method for the numerical solution of the generalized-Caputo type fractional differential equations. Math Comput Simul. 2024; 220: 462-80. https://doi.org/10.1016/j.matcom.2024.01.017

[37] Chauhan RP, Singh R, Kumar A, Thakur NK. Role of prey refuge and fear level in fractional prey-predator model with anti-predator. J Comput Sci. 2024; 81: 102385. https://doi.org/10.1016/j.jocs.2024.102385

[38] Almuallem NA, Chauhan RP. Effects of quarantine and vaccination on the transmission of Lumpy skin disease: A fractional approach. PLoS One. 2025; 20(7): e0327673. https://doi.org/10.1371/journal.pone.0327673

[39] Chauhan RP. Analyzing the memory-based transmission dynamics of coffee berry disease using Caputo derivative. Adv Theory Simul. 2025; e00373. https://doi.org/10.1002/adts.202500373

[40] Momani S, Chauhan RP, Kumar S, Hadid S. Analysis of social media addiction model with singular operator. Fractals. 2023; 31(10): 2340097. https://doi.org/10.1142/S0218348X23400972

[41] Li Z, Jiang W, Zhang Y. Dynamic analysis of fractional-order neural networks with inertia. AIMS Math. 2022; 7(9): 16889-906. https://doi.org/10.3934/math.2022927

[42] Wang Z, Zhang H. The role of neural inhibition in delayed recurrent neural networks. J Phys. 2006; 55(11): 5674-80.

[43] Podlubny I. Fractional differential equations: an introduction to fractional derivatives, fractional differential equations, methods of their solution and some applications. Elsevier; 1998.

[44] Sadabad MK, Akbarfam AJ, Shiri B. A numerical study of eigenvalues and eigenfunctions of fractional Sturm-Liouville problems via Laplace transform. Indian J Pure Appl Math. 2020; 51(3): 857-68. https://doi.org/10.1007/s13226-020-0436-2

[45] Diethelm K, Ford NJ, Freed AD. A predictor-corrector approach for the numerical solution of fractional differential equations. Nonlinear Dyn. 2002; 29: 3-22. https://doi.org/10.1023/A:1016592219341

[46] Li QY. Modern numerical analysis. Beijing: Higher Education Press; 1995.

[47] Diethelm K, Freed AD. The FracPECE subroutine for the numerical solution of differential equations of fractional order. Forschung Wiss Rechnen. 1998; 1999: 57-71.

[48] Huang C, Mo S, Cao J. Detections of bifurcation in a fractional-order Cohen-Grossberg neural network with multiple delays. Cogn Neurodyn. 2024; 18(3): 1379-96. https://doi.org/10.1007/s11571-023-09934-2

[49] Sun Q, Xiao M, Tao B. Local bifurcation analysis of a fractional-order dynamic model of genetic regulatory networks with delays. Neural Process Lett. 2018; 47: 1285-96. https://doi.org/10.1007/s11063-017-9690-7

[50] Wang H, Huang C, Liu H, Cao J. Detecting bifurcations in a fractional-order neural network with nonidentical delays via Cramer's rule. Chaos Solitons Fractals. 2023; 175: 113896. https://doi.org/10.1016/j.chaos.2023.113896

[51] Steven H. Nonlinear dynamics and chaos. Beijing: China Machine Press; 2016.